Airborne measurements of NO$_x$, tracer species, and small particles during the European Lightning Nitrogen Oxides Experiment

H. Huntrieser,[1] C. Feigl,[1] H. Schlager,[1] F. Schröder,[1] C. Gerbig,[2,3] P. van Velthoven,[4]
F. Flatøy,[5] C. Théry,[6] A. Petzold,[1] H. Höller,[1] and U. Schumann[1]

[1] Airborne in situ measurements of NO, NO$_2$, NO$_y$, CO, CO$_2$, O$_3$, J(NO$_2$), and CN were performed in European thunderstorms during the field experiment EULINOX in July 1998. The measurements in the upper troposphere show enhanced NO$_x$ (= NO + NO$_2$) concentrations within thunderstorms and their outflow at horizontal scales from 300 m to several 100 km. The maximum NO mixing ratio measured inside a thundercloud close to lightning (the aircraft was also hit by a small lightning strike) was 25 ppbv. A regional NO$_x$ enhancement of 0.5 ppbv over central Europe could be traced back to a thunderstorm event starting ∼24 hours earlier over Spain. The fractions of NO$_x$ in thunderclouds which are produced by lightning and convectively transported from the polluted boundary layer are determined by using CO$_2$ and CO as tracers for boundary layer air. The analyses show that on average about 70% of the NO$_x$ increase measured in the anvil region was found to result from production by lightning and about 30% from NO$_x$ in the boundary layer. Thunderstorms are also strong sources of small particles. The peak CN concentrations measured within thunderstorm outflows (>30,000 particles STP cm^{-3}) were distinctly higher than in the polluted boundary layer. The amount of NO$_x$ produced per thunderstorm and NO produced per lightning flash was estimated. The results imply that the annual mean NO$_x$ budget in the upper troposphere over Europe is dominated by aircraft emissions (0.1 TgN yr^{-1}) in comparison to lightning production (∼0.03 TgN yr^{-1}). On the global scale, NO$_x$ produced by lightning (mean 3 TgN yr^{-1}) prevails over aircraft-produced NO$_x$ (0.6 TgN yr^{-1}).   INDEX TERMS: 0320 Atmospheric Composition and Structure: Cloud physics and chemistry; 0322 Atmospheric Composition and Structure: Constituent sources and sinks; 0365 Atmospheric Composition and Structure: Troposphere—composition and chemistry; KEYWORDS: lightning, NO$_x$, thunderstorms, particle production

1. Introduction

[2] Nitrogen oxides (NO$_x$) have a strong impact on the chemistry in the atmosphere. In the troposphere, NO$_x$ acts as an important catalyst for the ozone production [*Liu*, 1977; *Jaeglé et al.*, 1999]. The impact of additional NO$_x$ is particularly large in the upper troposphere because the lifetime there is far longer than in the boundary layer. Lifetimes of about 5 days can be expected in summer at midlatitudes in the upper troposphere in comparison to a few hours in the boundary layer [*Ehhalt et al.*, 1992; *Davis et al.*, 1996; *Jaeglé et al.*, 1998]. In addition, the HO$_2$/OH partitioning in the upper troposphere is strongly dependent on NO [*Liu*, 1977].

Since all this affects the abundance of some greenhouse gases, the NO$_x$ concentration in the upper troposphere is one of the important factors controlling our climate [*Intergovernmental Panel on Climate Change* (*IPCC*), 1999].

[3] The production by lightning is considered to be one of the most important NO$_x$ sources in the upper troposphere [*World Meteorological Organization* (*WMO*), 1995; *Lamarque et al.*, 1996; *Bradshaw et al.*, 2000]. However, the uncertainties for lightning-produced NO$_x$ on the global scale are still large (range 2–20 Tg(N) yr^{-1}) in comparison to aircraft-produced NO$_x$ (range 0.5–0.6 Tg(N) yr^{-1}) since validations with in situ measurements are more difficult [*Logan*, 1983; *Lee et al.*, 1997; *Wang et al.*, 1998b; *Bradshaw et al.*, 2000]. Even less knowledge exists about the (probably) second most important NO$_x$ source in the upper troposphere, the upward transport of polluted planetary boundary layer (PBL) air [*Ehhalt et al.*, 1992]. This transport is controlled by the strong convection in the thunderstorm inflow area and by frontal lifting. In less than 1 hour a thunderstorm can transport PBL air into the upper troposphere [*Hauf et al.*, 1995; *Skamarock et al.*, 2000]. This source is most important when thunderstorms move over urban areas and may be neglected over oceans [*Corbett et al.*, 1999]. To separate the mixture of lightning-produced and PBL-transported NO$_x$ observed in thunderstorm anvils [*Ridley et al.*, 1996; *Winterrath et al.*, 1999], tracers for boundary layer air like O$_3$, CO, and CO$_2$ have been used in earlier studies [*Dickerson et al.*, 1987; *Pickering et al.*, 1996; *Ridley et al.*, 1996; *Huntrieser et al.*, 1998; *Dye et al.*, 2000]. However, not only upward transport of polluted PBL air can change the NO$_x$ abundance in

[1]Institut für Physik der Atmosphäre, Deutsches Zentrum für Luft- und Raumfahrt, Oberpfaffenhofen, Wessling, Germany.
[2]Institut für Chemie und Dynamik der Geosphäre, Forschungszentrum Jülich, Jülich, Germany.
[3]Now at Department of Earth and Planetary Science, Harvard University, Cambridge, Massachusetts, USA.
[4]Section of Atmospheric Composition, Royal Netherlands Meteorological Institute, De Bilt, Netherlands.
[5]Norwegian Institute for Air Research, Kjeller, Norway.
[6]Atmospheric Environment Research Section, Environnement Atmosphérique et Givrage du Département Mesures Physiques, Office National d'Etudes et de Recherche Aérospatiales, Chatillon, France.

the upper troposphere. Downward transport of NO_x-rich stratospheric air (stratospheric intrusion) can also enhance the upper tropospheric NO_x concentration (<1 Tg(N) yr^{-1}) [*Lee et al.*, 1997].

[4] A survey of estimates of lightning-produced NO_x from field measurements carried out in the last 20 years has been published recently by *Huntrieser et al.* [1998]. During most anvil penetrations reported so far, rather smooth NO_x enhancements (<2 ppbv, ppbv equal to parts per billion by volume) have been observed [e.g., *Chameides et al.*, 1987]. Occasionally, in addition, narrow NO spikes (∼4 ppbv) have been observed in the anvil region [*Dickerson et al.*, 1987; *Luke et al.*, 1992; *Stenchikov et al.*, 1996; *Huntrieser et al.*, 1998]. This spiky NO structure has been attributed to NO production by recent flashes [e.g., *Höller et al.*, 1999]. Recently, a large spike of 19 ppbv NO was measured in a thundercloud anvil during the field experiment STERAO in Colorado [*Stith et al.*, 1999; *Dye et al.*, 2000].

[5] In addition to single anvil penetrations, also extended lightning NO_x signatures have been observed on the regional scale. NO_x enhancements (up to 3 ppbv) extending over several hundreds of kilometers horizontally in the upper troposphere were observed frequently during the NOXAR experiment on flights between Switzerland and the United States or Asia, respectively [*Brunner et al.*, 1998; *Jeker et al.*, 2000]. It was shown that the NO_x concentration was proportional to the number of lightning flashes accumulated along the backward trajectories. The large-scale NO_x plumes were observed even 1−2 days after the convection. During SONEX, also several episodes with extended NO_x plumes in the upper troposphere were observed which were partly related to the production by lightning [*Crawford et al.*, 2000]. The initial NO_x concentrations in these plumes were estimated to vary between 1 and 7 ppbv. It was concluded that these lightning NO_x episodes have a large impact on the average NO_x concentration in the upper troposphere. *Crawford et al.* [2000] and others [e.g., *Clarke et al.*, 1998] also reported formation of new particles (ultrafine condensation nuclei) in the convective outflow. During the POLINAT experiment in the North Atlantic flight corridor [*Schumann et al.*, 2000], an extended NO_x plume in the shape of a thin widespread cirrus cloud was found during one flight which was traced back to be the remnant of thunderstorms active 24 hours before over Spain [*Huntrieser et al.*, 1996]. *Ström et al.* [1999] found that widespread cirrus clouds containing enhanced NO_x concentrations due to convection can have an important effect on O_3. Furthermore, *Smyth et al.* [1996] found wide pronounced NO plumes (up to 0.8 ppbv extending over 100−1000 km) during the TRACE-A experiment in the South Atlantic, which they related to production by lightning and convective transport of emissions from biomass burning.

[6] The source strength of lightning-produced NO_x needs to be known on various scales for predicting future developments of tropospheric ozone and climate. The effect of aircraft emissions on tropospheric ozone cannot be assessed properly without accounting for lightning NO_x sources [*Beck et al.*, 1992; *Pickering et al.*, 1993; *Brasseur et al.*, 1996; *Berntsen and Isaksen*, 1999; *Lelieveld and Dentener*, 2000]. Chemical transport model (CTM) calculations show that lightning emissions can cause a local O_3 increase of 20 ppbv [*Flatøy and Hov*, 1997; *Stockwell et al.*, 1999]. A lightning rate increase of 4% per year as found by *Orville* [1994] could increase the global rate of lightning-produced NO_x by 0.16 Tg(N) yr^{-1}, which is distinctly more than the increase rate of aircraft NO_x emission [*Bradshaw et al.*, 2000, also unpublished manuscript, 1996]. In comparison, *Michalon et al.* [1999] estimated a 10% increase in lightning frequency for a surface warming of 2 K. Recent investigations of Optical Transient Detector (OTD) satellite data by *Reeve and Toumi* [1999] predict that a change in global wet-bulb temperature of 1 K would increase global lightning activity by 40%. These recent findings show the importance of better understanding lightning-produced NO_x.
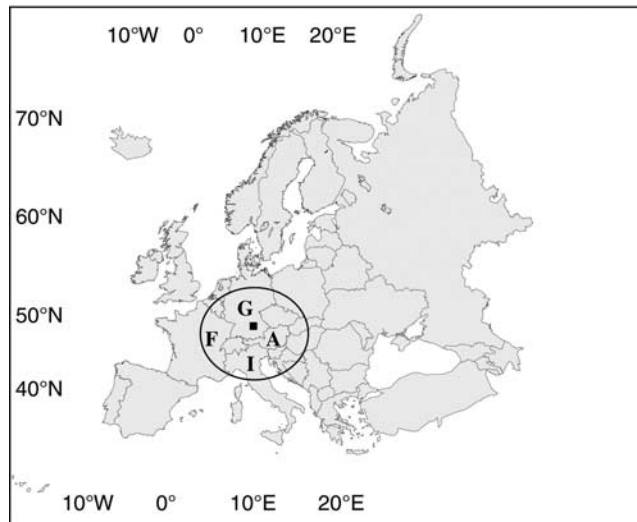

Figure 1. Map showing Europe and the area of the airborne measurements (within the circle). The solid square indicates the location of the DLR operation center (Oberpfaffenhofen near Munich). G, Germany; F, France; A, Austria; I, Italy.

[7] In order to reduce some of the uncertainties listed above, the European Lightning Nitrogen Oxides (EULINOX) project was conducted with a field campaign in July 1998. The experiment was coordinated by the Deutsches Zentrum für Luft- und Raumfahrt (DLR) located in Oberpfaffenhofen near Munich in southern Germany (48°N, 11°E). The experiment was performed jointly with Forschungszentrum Jülich (FZJ), Koninklijk Nederlands Meteorologisch Instituut (KNMI), Norsk institutt for luftforskning (NILU), and Office National d'Etudes et de Recherches Aérospatiales (ONERA), and funded by the European Commission. Further details are given in the EULINOX project report [*Höller and Schumann*, 2000]. The main objective of EULINOX was to estimate the importance of lightning-produced NO_x in comparison to other sources in the atmosphere, in particular aircraft emissions. In this paper the lightning source is estimated on various scales, based on local and mesoscale thundercloud in situ observations, and extrapolated to the European and the global scale. During eight EULINOX flights more than 10 different electrically active or inactive convective storms were penetrated by the DLR Falcon research aircraft. Further, the outflow from distant convective systems was penetrated. In section 2 the research flights and the instrumentation, which was used to study the chemistry and electrification in the thunderstorms, are described briefly. The results of the in situ trace gas measurements are presented in section 3. Estimates of the contribution of lightning-produced NO_x to the European and global nitrogen budget are given in section 4. Section 5 summarizes the EULINOX results.

2. Field Experiment and Data Availability

[8] The airborne measurements during EULINOX were performed with two DLR research aircraft, the jet aircraft Falcon, operating mainly in the upper troposphere (7−10 km), and a turboprop aircraft of type Dornier-228 (DO-228) for boundary layer observations (<4 km). The Falcon performed flights over the whole of central Europe (Figure 1) on 1, 3, 7, 10, 14, 17, 20, and 21 July. The DO-228 performed only five local flights close to the operation site on 10, 15, 20, 21, and 23 July. The DO-228 aircraft was equipped with instruments to measure O_3 (available for 10, 15, 20, 21, and 23 July), CO_2 (available only for 10, 15, 21, and 23 July), and NO (available only for 10, 15, 20, and 23 July). The

Table 1. Falcon Instrumentation

Species	Technique	Detection Limit	Sampling Rate, s	Accuracy, %	Group	Reference
NO	chemiluminescence (CL)	3 ppt	1	5 (for 0.2 ppb)	DLR	*Schlager et al.* [1997], *Feigl* [1998], *Ziereis et al.* [1999]
NO_2	photolytic converter plus CL	15 ppt	5	10 (for 0.2 ppb)	DLR	*Schlager et al.* [1997], *Feigl* [1998], *Ziereis et al.* [1999]
NO_y	Au-converter plus CL	50 ppt	1	15 (for 0.2 ppb)	DLR	*Feigl* [1998]
O_3	UV absorption	1 ppb	5	5	DLR	*Schlager et al.* [1997], *Huntrieser et al.* [1998]
CO	VUV fluorescence	2 ppb	1	3	FZJ	*Gerbig et al.* [1996], *Gerbig et al.* [1999]
CO_2	NDIR	1 ppm	1	0.3	DLR	*Schulte et al.* [1997]
$J(NO_2)$	Filter radiometry	$1E\text{-}4,^{a} s^{-1}$	1	6	DLR	*Volz-Thomas et al.* [1996], *Beine et al.* [1999], *Shetter and Müller* [1999]
CN	CNC (size 10 nm to 1 μm)	10 nm	1	...	DLR	*Schröder et al.* [1998]

[a] Read 1E-4 as 1×10^{-4}.

DO-228 measurements of O_3 were used to extend the Falcon measurements to lower altitudes since Falcon O_3 measurements were not available in the PBL. It was planned to use the DO-228 aircraft to characterize the conditions in the PBL ahead of thunderstorms (inflow) when the Falcon investigated the outflow. These kind of coordinated flights are difficult and were only allowed in a special observation area close to the operation site. One successful comparison flight for CO_2, O_3, and NO (wing-by-wing, no thunderstorms) was performed on 10 July, which, however, will not be discussed here. The second coordinated flight was performed on 21 July. The Falcon investigated an isolated thunderstorm, and the DO-228 flew ahead of the storm in the inflow area. Unfortunately, the DO-228 NO instrument was not operating on this day because of technical problems; however, the O_3 and CO_2 instruments were operating. For the reasons mentioned above, this paper focuses mainly on the measurements from the Falcon. The chemical and particle instrumentation in the Falcon is presented in Table 1. For a more precise description of the instrumentation, which has been used in several previous field experiments, see publications by *Schlager et al.* [1997], *Schulte et al.* [1997], *Feigl* [1998], *Huntrieser et al.* [1998], *Schröder et al.* [1998], and *Ziereis et al.* [1999] as listed in Table 1. The publication by *Feigl* [1998] describes the set up and the performance of the EULINOX NO_x and NO_y instrumentation in detail. The efficiency of the NO_2 converter was 0.64.

[9] All instruments are capable of measuring at high temporal resolution (1–5 s), allowing for the resolution of the often very small spatial structures of trace distributions in convective clouds. However, as mentioned before, no Falcon O_3 measurements could be made in the PBL. This was also the case on many days for the Falcon NO, NO_2, NO_y instrumentation when the PBL was too humid. Condensation on the cooled photomultiplier window had to be avoided. The instruments allow separation between NO and NO_2. Only the sum NO_x is approximately conserved during vertical transport. Fresh lightning emissions are mainly in the form of NO; however, the equilibrium between NO and NO_x is reached rather quickly (in minutes). Hence the ratios NO/NO_x, NO/NO_y, and NO_x/NO_y are a measure for the age of freshly produced NO in thunderclouds. Owing to the more complete NO and NO_x data set (in comparison to the NO_y data set), this paper concentrates mainly on the NO and NO_x measurements. It should be mentioned that the investigated thunderstorms were free from fresh aircraft-produced NO_x since airliners avoid flying through thunderstorms.

[10] The CO instrument was designed for EULINOX and used there for the first time. Details on the measuring technique are given by *Gerbig et al.* [1996, 1999]. In addition, two $J(NO_2)$ radiometers (upward and downward looking sensors) were newly included on the Falcon. The radiometers are manufactured by MeteoConsult, Glashütten (Germany), and measure the 4π solar actinic flux in the 300–380 nm spectral band. Corrections applied to the $J(NO_2)$ signals (due to spectral and angular response, altitude, solar zenith angle, and temperature) are described by *Volz-Thomas et al.* [1996], *Beine et al.* [1999], and *Shetter and*

Müller [1999]. Position, altitude, temperature, humidity, pressure, and wind (u, v, w) were measured with the standard Falcon meteorological measurement system [see *Schumann et al.*, 1995, 2000]. All altitude values refer to height above sea level, and all clock times refer to UTC.

[11] The total three-dimensional (3-D) distribution of lightning activity (100 km around the DLR operation center), in terms of intracloud (IC) and cloud-to-ground (CG) flashes, was registered by a measuring system provided by ONERA. It includes two remote Very High Frequency (VHF) interferometric stations measuring the direction of incoming VHF signals from lightning flashes at 114 MHz, with a 1 MHz bandwidth. The antenna were installed 50 km apart on a roughly northeast-southwest baseline, and they were nearly equidistant to the DLR operation center [*Höller and Schumann*, 2000]. The allocation error of the system for single flashes was 1–2 km. The same system was used in the Stratospheric-Tropospheric Experiment: Radiation, Aerosols, and Ozone (STERAO)-Deep convection experiment [*Defer et al.*, 2001]. The horizontal positions and times of lightning events (mainly CG lightning) were also registered with the German two-dimensional (2-D) Lightning Position and Tracking System (LPATS) [*Finke and Hauf*, 1996]. In addition, the European Arrival Time Difference (ATD) lightning system that registers the location and intensity of sferics was used (operated by the UK Met Office; for further details, see http://www.torro.org.uk/sfinfo.htm). Central European radar composites were delivered by the German Weather Service (DWD). Thunderstorms close to the operation site were monitored from the ground with the DLR polarimetric Doppler radar (POLDIRAD) [*Höller et al.*, 1994, 1999]. Lightning data from the LPATS and the ATD system, and radar data from the German Weather Service, are available daily for July 1998. However, lightning data from the VHF system, radar data from POLDIRAD, and aircraft measurements are only available for the EULINOX thunderstorm investigated on 21 July close to the operation site. The present paper will not focus on lightning and radar data during EULINOX since these analyses have already been carried out in separate publications [*Dotzek et al.*, 2000; *Höller et al.*, 2000; *Höller and Schumann*, 2000].

[12] For further analysis of the EULINOX data a suitable tracer had to be found for PBL air to distinguish lightning-produced NO_x from convectively transported PBL NO_x. During the LINOX experiment we found that CO_2 shows a more pronounced profile and is more suitable as PBL tracer than O_3 in our region [*Huntrieser et al.*, 1998]. During EULINOX, CO was also measured and used as an additional tracer for PBL air. However, due to technical problems, the instrument was only operating during the first flights (1, 3, and 7 July). The vertical CO distribution shows a pronounced profile with the highest concentrations in the PBL (due to pollution) decreasing with altitude which makes CO useful as tracer. However, since no CO data are available for several EULINOX flights (10, 14, 17, 20, and 21 July), we use mainly CO_2 as tracer for PBL air in this study. Depending on timescale, season, and region, CO may be a more useful PBL tracer than CO_2 since it has a source distribution more similar to NO_x.

Table 2. Brief Overview of EULINOX Aircraft Missions

Date	Time, UTC	Tropopause Height, km	Mission	Observations
1 July	1457–1639	10.8	test flight to France	enhanced NO_x in the upper troposphere (0.5 ppbv)
3 July	1448–1727	9.7	regional flight to Switzerland	penetration of several convective clouds with and without lightning (up to 6 ppbv NO, spiky signatures)
7 July	1036–1320	10.6	long-range flight to Yugoslavia	front penetration and penetration of isolated thunderstorms ahead of the cold front (up to 9 ppbv, spiky signatures)
10 July	1300–1534	11.3	intercomparison flight	trace gas measurements were compared (Falcon/DO-228)
14 July	1028–1334	10.9	long-range flight to Hungary	front penetration (0.5 ppbv NO, smooth signatures)
17 July	1424–1635	10.5	regional flight to Austria	penetrations of a squall line (up to 4 ppbv NO, few spiky signatures)
20 July	1407–1632	10.5	regional flight to Austria	penetration of small isolated thunderstorms (up to 1 ppbv NO, few spiky signatures)
21 July	1641–1849	10.2	regional flight near Munich	penetrations of a supercell (up to 25 ppbv NO, many spiky signatures)

[13] During the summer months, thunderstorms can be expected every second day on average in southern Germany [*Hagen et al.*, 1999]. During the EULINOX period from 29 June to 26 July 1998, research flights with the Falcon were performed on 8 days. Small-scale and mesoscale structures of individual convective cells in southern Germany were investigated in five flights. Flights across larger regional scales in central Europe (Germany, France, Italy, Switzerland, Austria, Yugoslavia, and Hungary) were performed in three missions (see Figure 1 and Table 2). A brief overview of the single aircraft missions (observations and tropopause height) is presented in Table 2. Some of the missions (1, 3, 17, and 21 July) will be discussed in more detail in section 3 (including area and altitude of the observed NO_x abundance).

3. Observed NO_x Signatures at Different Scales

[14] During EULINOX more than 10 different convective clouds were penetrated, some of them several times (together almost 40 penetrations). The convective cells had different characteristics. Some of them were isolated, and some of them were embedded in larger convective clusters or cold fronts. The convective clouds were penetrated in different stages of development including the growing stage characterized by a cumulus congestus cloud. In this stage, almost no or very little lightning is occurring (mainly IC), and no anvil is visible. In the mature stage some of the convective clouds grew to a cumulonimbus which developed an anvil. Often high lightning frequencies were observed at this stage, but some clouds were without lightning, possibly because of different cloud top altitudes and microphysics [*Price et al.*, 1997]. In the dissipating stage of the clouds the updraft ceases, and the lower and middle parts of the cloud rain out and eventually evaporate. The anvil of the cloud often develops into a wide, thin cirrus shield in the upper troposphere, which may spread over hundreds of kilometers and persist for several hours [*Waliser et al.*, 1993].

[15] During the EULINOX missions all the different convective clouds described above were penetrated. Observations for a large variety of convective clouds help to distinguish between NO_x produced by lightning and NO_x transported upward from the PBL by the convection (see sections 3.2.2 and 3.2.4). The measurements were separated according to events observed on different atmospheric scales and divided into regional scale signatures (>100 km, convective cold fronts, extended thunderstorm clusters, and thundercloud remnants) described in section 3.1, mesoscale signatures (1–100 km, electrically active and inactive convective clouds) described in section 3.2, and microscale signatures (<1 km, near lightning channels) described in section 3.3. Depending on the atmospheric scale, different NO_x concentrations were measured with the highest concentrations on the microscale (fresh NO_x) and the lowest on the regional scale as expected from the dilution as well as from the increasing age of the NO_x in the sample. To get a complete picture of the influence of thunderstorms on the upper troposphere over Europe, at least one case representing every scale

is described in the paper. The regional scale case described below shows a typical NO_x plume over central Europe that has been observed before in similar studies over Europe [e.g., *Huntrieser et al.*, 1996, 1998]. However, in this paper for the first time more detailed information is also given for other trace gases like CO, CO_2, O_3, and also CN (including mean vertical profiles during EULINOX), and the observations were accompanied by CTM simulations. The described mesoscale and microscale thunderstorm observations in the second and third section are unique and have never been observed in such detail over Europe before.

3.1. NO_x Signatures on the Regional Scale

[16] During the first EULINOX mission on 1 July the Falcon flew to the west to sample an area close to Basel (border France/Switzerland). The day before the flight, forward trajectories had been started by KNMI from a large thunderstorm cluster active over northern Spain in the afternoon and evening. It was predicted that air advected from this cluster would reach the French/Swiss border 24 hours later. The main part of the flight was performed in the upper troposphere. During the ascent into the tropopause region (located between 10.8 and 11.4 km) close to Basel, the Falcon actually observed an extended layer (between 9 and 10 km) with enhanced NO_x concentrations (∼0.5 ppbv, described in detail in section 3.1.3) in cloud-free air several hundreds of kilometers downwind of the active thunderstorm cluster that at this time reached central France.

3.1.1. Meteorological conditions for 1 July 1998. [17] In order to explain where and how the expected convective transport took place in more detail, 5-day backward trajectories were used. The trajectory calculations were performed by KNMI using analyses from the European Centre for Medium-Range Weather Forecasts (ECMWF; horizontal resolution 40 km). Every 30 min of the flight 15 backward trajectories were put together in one picture like in Figure 2 (one trajectory every 2 min of the flight). The time period shown in Figure 2 covers the period of the trace gas signatures at 9–10 km described before. The major part of the trajectories are tightly bounded when followed 1 day back, and the origin area of this air mass can be identified easily. This suggests that the air sampled at 9–10 km originated from a thunderstorm event that started 24 hours earlier over northeastern Spain. The vertical motion of the trajectories (not shown) indicates a large-scale lifting of the trajectories from the lower-mid to the upper troposphere starting over Spain about 24 hours before the flight.

[18] The infrared (IR) image of the Meterological Satellite (METEOSAT) at 0000 UTC on 1 July shows a large thunderstorm cluster active over the northern part of Spain (Figure 3a) which developed from several single thunderstorm cells in the afternoon on 30 June. The European ATD lightning detection network registered high lightning frequencies between 16 UTC and mid-night on 30 June over the whole of northern Spain with maximum intensities of 16–24 strikes min^{-1} at several locations. The next day (1 July) the complex moved to France and was not very active in the morning and early afternoon. However, in the late afternoon
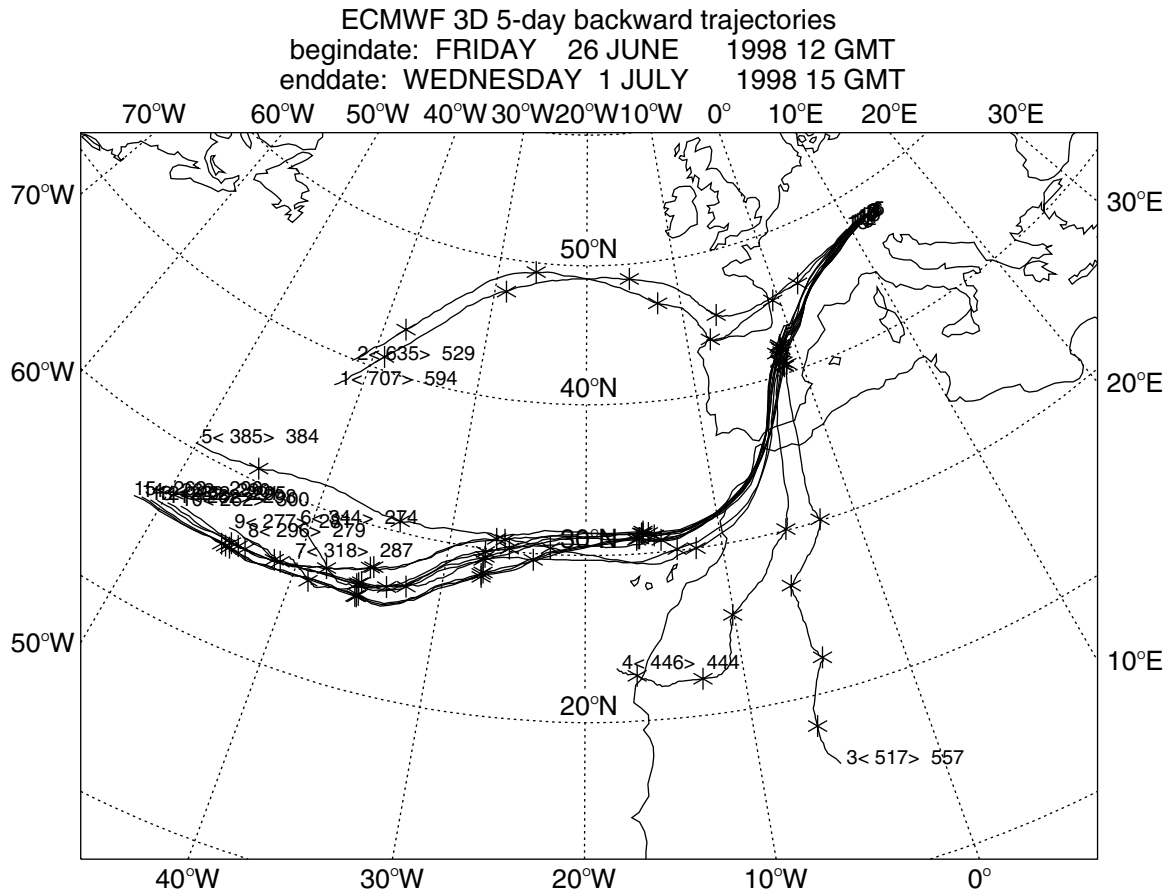
Figure 2. Backward trajectories (5 days) calculated by KNMI for 1 July, 1530–1558 UTC. Trajectories were calculated backward every 2 min along the flight track over a 5-day period. One day travel time is marked with an asterisk.
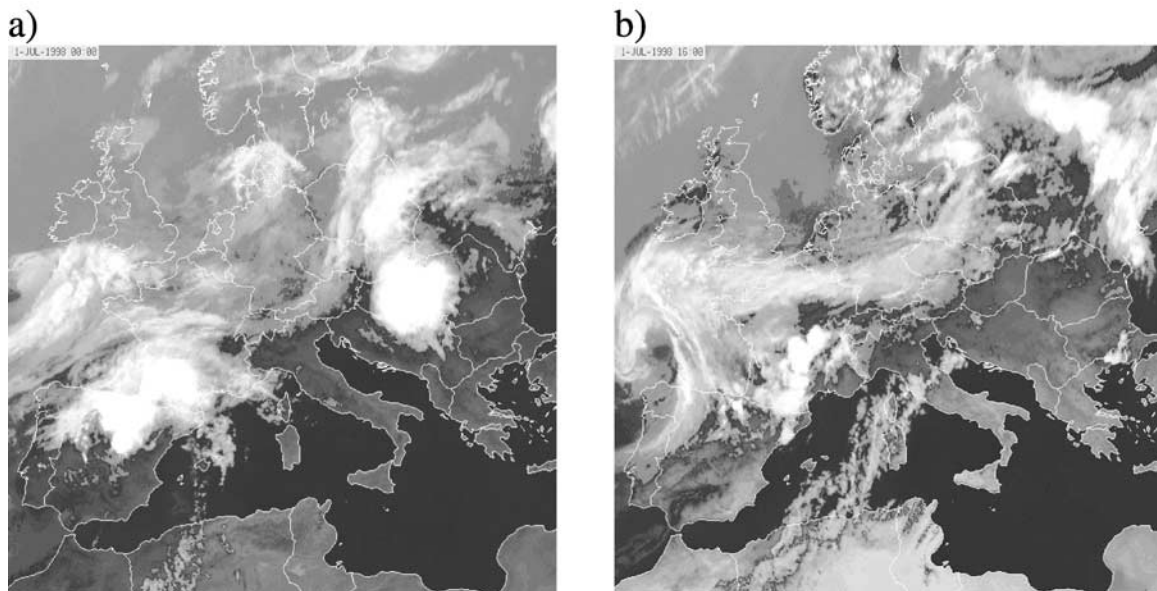

Figure 3. METEOSAT-IR images: (a) 0000 UTC, 1 July and (b) 1600 UTC, 1 July showing among others a large thunderstorm cluster over Spain and France moving in a northeast direction.
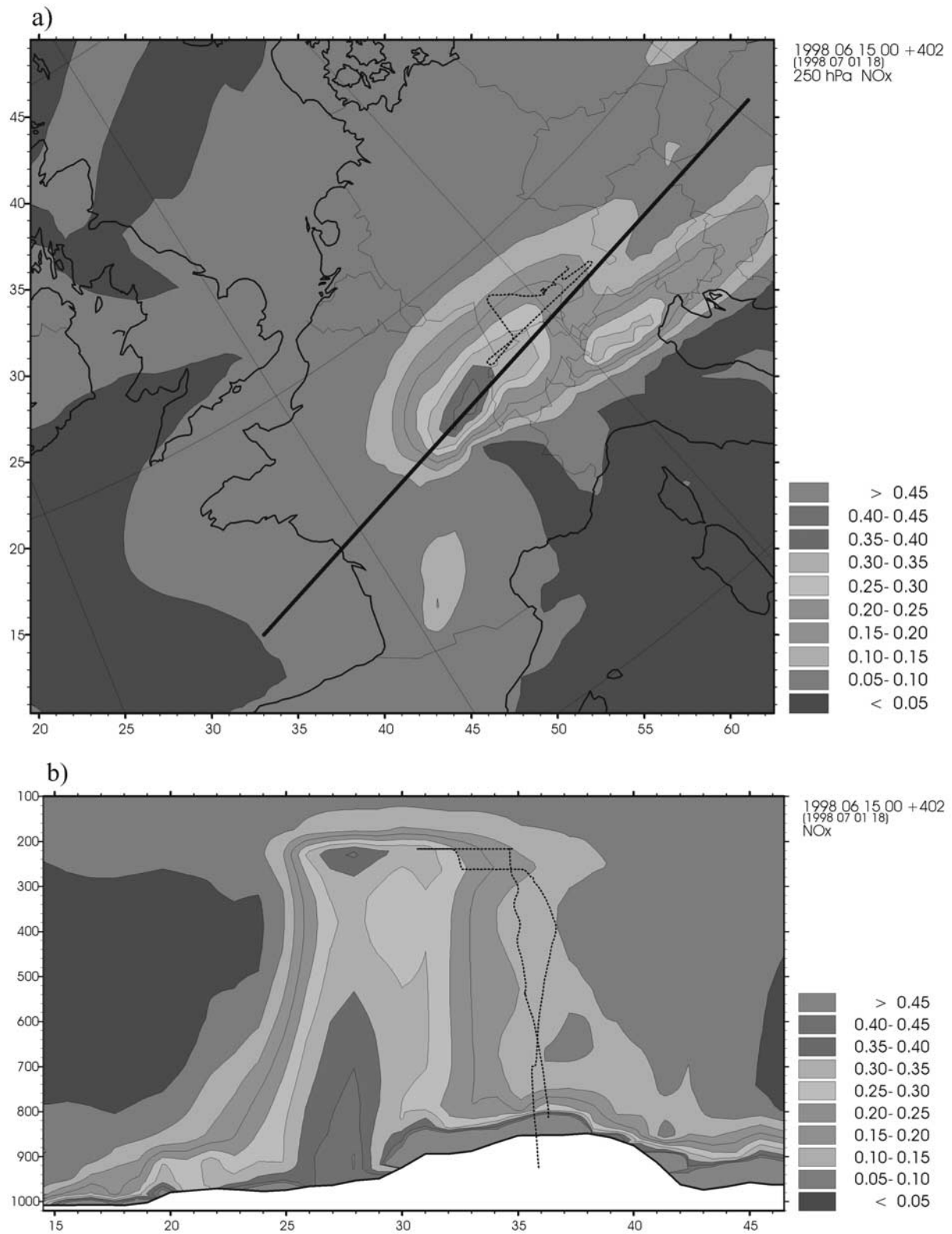
Figure 4. CTM calculation from NILU for 1800 UTC 1 July. (a) Total horizontal NO_x distribution (ppbv) at 250 hPa over western Europe (including lightning-produced NO_x). (b) Total NO_x distribution in a cross section along the line indicated in Figure 4a. The dotted lines in all figures indicate the flight track. See color version of this figure at back of this issue.
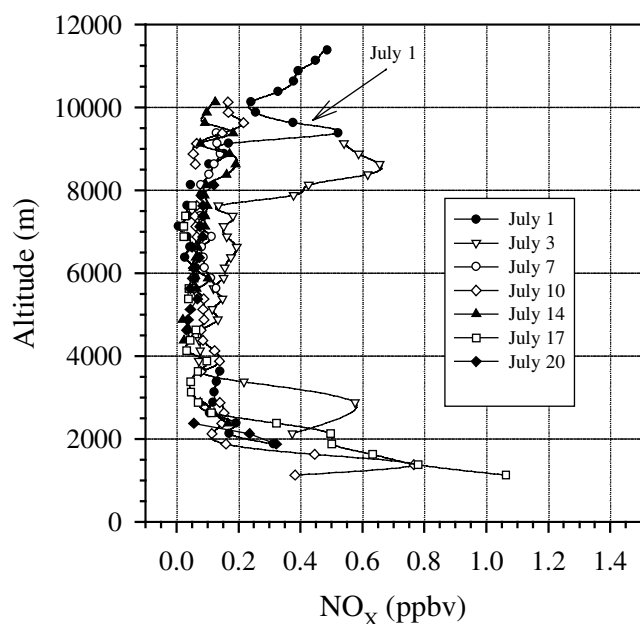
Figure 5. Observed vertical NO$_x$ distribution (in ppbv) on single EULINOX mission days indicated by different symbols (single cloud penetrations excluded).

the lightning activity increased again. The flight to the west in the afternoon passed a dry area ahead of the storm system which explains why the observed NO$_x$ enhancement close to Basel (French/Swiss border) was not connected with any visible clouds (Figure 3b).

3.1.2. Chemical transport model calculations for 1 July 1998. [19] Chemical Transport Model (CTM) calculations by NILU [*Flatøy et al.*, 2000] support the findings that convective transport and NO$_x$ production by lightning perturbed the trace gas composition in 9–10 km altitude over mid Europe on 1 July (Figures 4a–4b). The CTM is driven by meteorological data from a Numerical Weather Prediction (NWP) model using global meteorological analyses and forecasts from ECMWF as initial and boundary conditions. Figure 4a shows the simulated horizontal NO$_x$ distribution over western Europe at 250 hPa for 1800 UTC (2 hours later than the flight mission which is the closest simulation to the flight). An elongated area with enhanced NO$_x$ is visible west of Basel, Switzerland. The black line indicates the axis of the vertical cross section that is presented in Figure 4b. The vertical NO$_x$ distribution shows clearly the effect of the thunderstorm complex visible in the satellite images. There is strong upward pumping of polluted boundary layer air and a distinct outflow in the upper troposphere. The CTM result includes the NO$_x$ enhancement due to production by lightning. The parameterization of lightning emissions is based on the modeled convection (function of the cloud thickness and the intensity of latent heat generation); for further details, see *Flatøy and Hov* [1997]. The Falcon penetrated the convective outflow area (thin dotted black line in Figure 4b) which explains the measured enhanced NO$_x$ concentration in the range of 0.2–0.5 ppbv in 9–10 km altitude (see Figure 5). The CTM simulations gave concentrations of the same order, about 0.30–0.35 ppbv NO$_x$. The horizontal extension of this NO$_x$ abundance covers at least 500 km, and it probably contains fresh NO$_x$ from the thunderstorms over France mixed with 1-day-old NO$_x$ from the thunderstorms over Spain as indicated by the trajectory analysis. The CTM simulations also showed an increased ozone production rate of 1 ppbv h^{-1} in the NO$_x$ plume which has an important effect on chemistry in the upper troposphere.

[20] The 1 July event is interesting and different from all other EULINOX thunderstorms. The thunderstorm cluster on 30 June and 1 July was large enough to be resolved by the ECMWF analysis data used for both the CTM and the trajectory calculations. Still, the model and the use of ECMWF vertical winds are inappropriate to resolve the small-scale updrafts in thunderstorms and vertical motions of the trajectories in the thunderstorm complex [see also *Hannan et al.*, 2000].

3.1.3. Vertical NO$_x$ profiles during EULINOX and focusing on 1 July 1998. [21] In order to compare the relevance of this processed thunderstorm air with more common conditions the vertical trace gas profiles from 1 July were plotted together with other trace gas profiles obtained during EULINOX. In Figure 5 the vertical NO$_x$ distributions measured during seven EULINOX flights (except the 21 July flight) are presented. The observations from 21 July will be discussed separately in section 3.3. The symbols in Figure 5 indicate smoothed average values every 250 m. Each presented vertical profile includes all data from one flight. Therefore the vertical profile is an average profile for a larger region covered by the Falcon. This is true especially for the average values in the upper troposphere (main cruise altitude). The average values obtained for the middle and lower troposphere are close to the operation site after start and before landing. The vertical profiles represent background conditions outside of convective clouds. Measurements during cloud penetrations were excluded to avoid direct interference from fresh lightning-produced or transported NO$_x$ within the clouds (this was done for almost all vertical profiles presented in this paper, except profiles from 21 July and partly 3 July).

[22] The typical C shape of the vertical NO$_x$ distribution can be noticed with high concentrations in the boundary layer and increasing concentrations toward the tropopause region. Unfortunately, only one flight (1 July) was performed in the tropopause region (above 10 km), and no flight was performed in the stratosphere. However, previous flights in the northern European area during summer by our group also show the typical increase within the lowermost stratosphere [e.g., *Zierers et al.*, 1999, 2000]. On some of the EULINOX days, especially 1 and 3 July, the NO$_x$ concentration in the upper troposphere is distinctly higher than expected from the typical C-shape profile due to lightning-produced NO$_x$ and transported NO$_x$ from the PBL. In the next sections the impact of the vertical transport on other chemical species is presented. The results can be compared to a recent study by *Wang and Prinn* [2000]; see Figure 8 in this reference.

3.1.4. Vertical CO, CO$_2$, and O$_3$ profiles during EULINOX and focusing on 1 July 1998. [23] CO, CO$_2$, and O$_3$ undergo slow chemistry compared to vertical transport in thunderstorms and can therefore be used as tracers. The origin of the air masses and related NO$_x$ sources can be estimated. Figure 6a shows the vertical CO distribution on 1 July. Unfortunately, almost no data are available in the boundary layer. Usually, the CO mixing ratio decreases with altitude over the European continent as shown in the mean profile in Figure 6b and as shown by *Gerbig et al.* [1996] over Portugal. On 1 July a local CO increase is visible between 9 and 10 km indicating convective transport from lower altitudes, which partly can explain the observed NO$_x$ enhancement in this layer (besides lightning-produced NO$_x$). Only one flight (1 July) was performed above 10 km which is the reason for the lack of standard deviations above this altitude (in Figure 6b also around 4 km).

[24] Vertical CO$_2$ concentration profiles are shown in Figures 6c–6d. A small CO$_2$ decrease is visible in the profile between 9 and 10 km (Figure 6c), consistent with the suggested convective transport. The mean vertical profile of CO$_2$ (Figure 6d, black-dotted profile) is found as expected for the summer season over central Europe with increasing concentration with altitude. Above the tropopause the CO$_2$ concentration decreases (no EULINOX measurements available). The CO$_2$ difference between the free
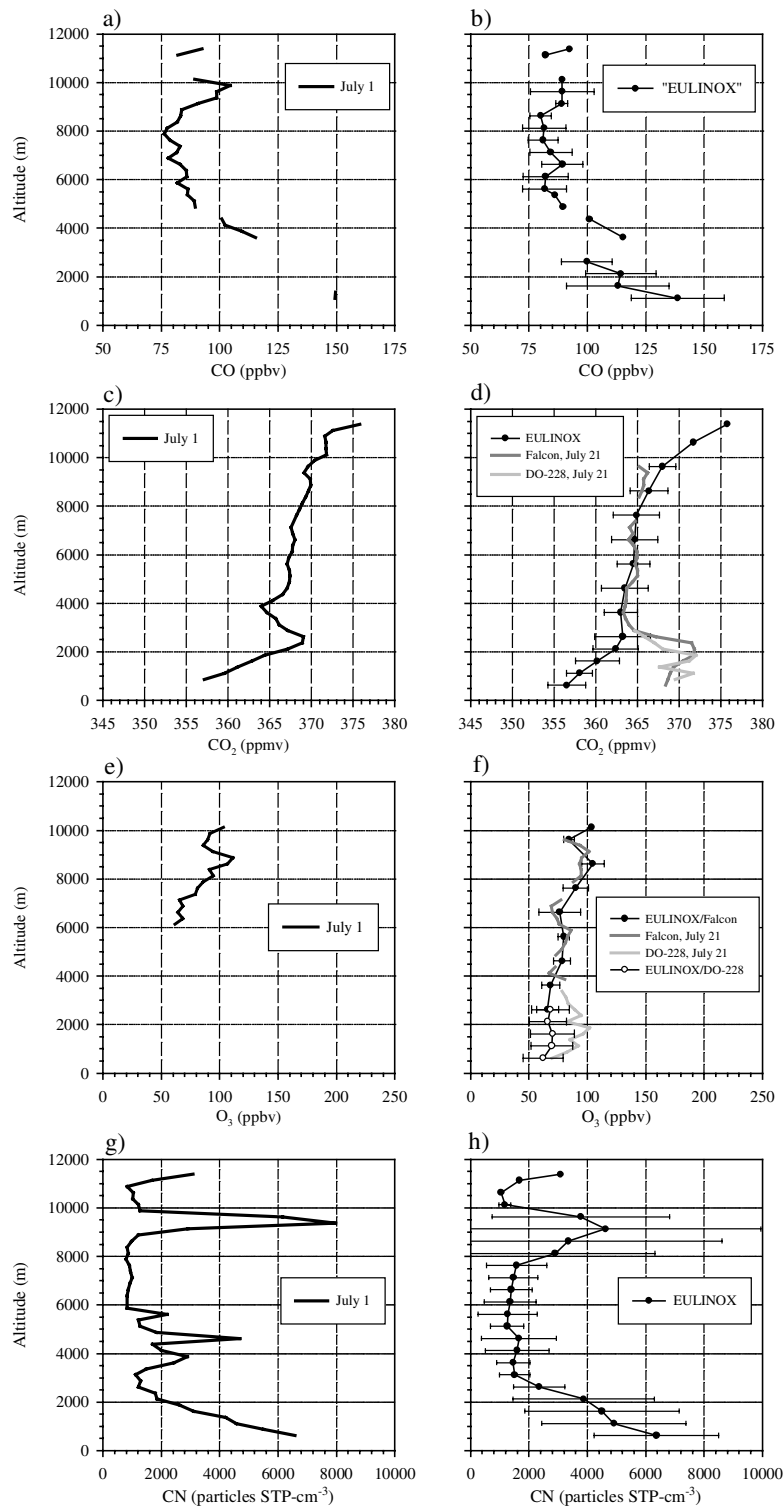
Figure 6. (a) Vertical CO profile on 1 July and (b) mean profile and standard deviation (bars) determined by averaging the CO data from the EULINOX mission days 1, 3, and 7 July. (c) Vertical CO_2 profile on 1 July and (d) mean profile (lines with symbols) and standard deviation (bars) determined by averaging the CO_2 data from all EULINOX mission days (except 21 July). The gray lines in Figure 6d show the vertical CO_2 profile on 21 July measured by the Falcon (dark gray) and DO-228 (extremely polluted PBL). (e) Vertical O_3 profile on 1 July. (f) Black line with solid dots is the mean vertical O_3 profile estimated by averaging the ozone data from all EULINOX-Falcon mission days (except 21 July). Black line with open dots is the mean vertical O_3 profile determined by averaging the ozone data from all EULINOX-DO-228 mission days (except 21 July). Horizontal bars indicate the standard deviation. Gray lines show the vertical O_3 profile on 21 July (extremely polluted PBL). (g) Vertical CN profile (number of particles cm^{-3} at standard pressure and temperature) on 1 July and (h) mean profile and standard deviation (bars) determined by averaging the CN data from all EULINOX mission days (except 21 July).
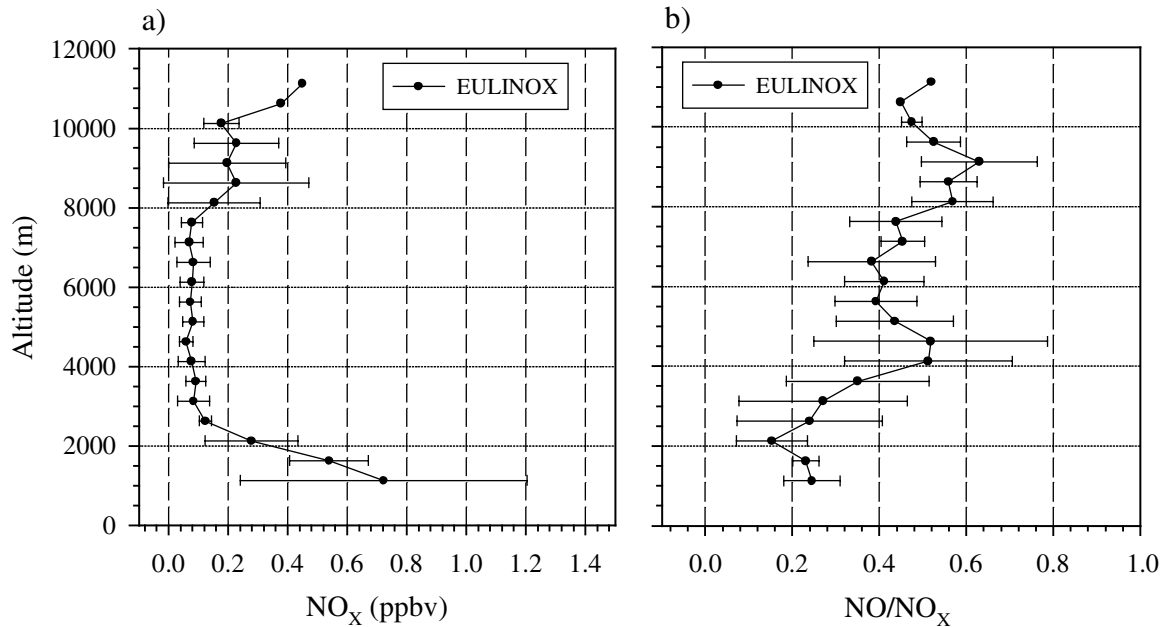
Figure 7. Average profiles of (a) NO_x concentration and (b) NO/NO_x ratio. The profiles represent the mean values from all EULINOX mission days (except 21 July). The horizontal bars indicate the standard deviation.

troposphere and the PBL is about 10 ppmv and hence larger than the standard deviation. The concentration is lower in the boundary layer because of CO_2 uptake by vegetation (photosynthesis) in the summer season, especially after noon, when the flights were performed [*Anderson et al.*, 1996; *Denning et al.*, 1996, Figure 7; *Bakwin et al.*, 1998]. This difference in CO_2 mixing ratio can be used to identify convective transported air masses from the boundary layer into the upper troposphere. Figure 6d also shows the vertical profile measured on 21 July (gray profile). This day was very exceptional with no CO_2 minimum in the boundary layer. Instead, a pronounced maximum is visible which indicates that the air was strongly polluted by combustion products.

[25]   As a third tracer, Figures 6e and 6f show the vertical O_3 distribution. On 1 July, O_3 measurements are available for the upper troposphere only. A small O_3 decrease is visible between 9 and 10 km (Figure 6e), which may be caused by convective transport, if the shape of the vertical profile over Spain is similar as shown in Figure 6f for EULINOX. The O_3 mixing ratio is slightly increasing with altitude, similar to the observed CO_2 profiles. DO-228 data are used to extend the O_3 profile into the PBL.

3.1.5.   Vertical CN profiles during EULINOX and focusing on 1 July 1998. [26]   The CN concentration is given for standard conditions at $0°C$ and 1013 hPa (STP cm^{-3}) so that it is a conserved property during vertical motions. The mean profile of the condensation nuclei (CN) particle concentration (particles between 10 nm and 1 μm diameter) measured during EULINOX shows a large variability (standard deviation) in the PBL and in the upper troposphere (Figure 6h). The variability in the upper troposphere even exceeds the concentration means observed in the PBL. This indicates that particles can be produced in thunderclouds (possibly also due to lightning; see section 3.3.3). On 1 July (Figure 6g) a tongue with enhanced particle concentration (almost 10,000 particles STP cm^{-3}) was found between 9 and 10 km which coincides with the NO_x enhancement.

3.1.6.   Discussion of the mean vertical trace gas distributions during EULINOX. [27]   In order to generalize the findings from the 1 July case, where a pronounced NO_x enhancement was observed in the cloud outflow region, the mean vertical NO_x profile (including standard deviation) obtained during the

EULINOX campaign is shown in Figure 7a. Only one flight (1 July) was performed above 10 km which is the reason for the lack of standard deviations above this altitude. The C shape mentioned before is also visible in the mean. The large scatter in the PBL is caused by varying anthropogenic surface sources and surface winds. The NO_x abundance with large standard deviations in the upper troposphere (8–10 km, just below the tropopause) may result from convective transports from the surface and from lightning, which occurred often in July 1998, and additionally from aircraft emissions. *Jeker et al.* [2000] also found a distinct NO_x maximum (0.3 ppbv) just below the tropopause during the NOXAR experiment. Even coupled chemistry-climate models indicate this NO_x maximum 2–3 km below the tropopause [*Grewe et al.*, 2001]. The C shape of the vertical NO_x profile is replaced by an "E-shaped" profile with a local maximum in the upper troposphere. Vertical NO_x profiles from the winter season do not show this high variability in the upper troposphere [*Ziereis et al.*, 1999; *Grewe et al.*, 2001]. Therefore the impact from aircraft emissions is probably minor in comparison to production by lightning in July. The NO_x variability observed in the upper troposphere (Figure 7a) is not caused by changes in tropopause height which was rather constant at 10–11 km during the flights (Table 2). The enhanced mean NO/NO_x ratio at 8–10 km during EULINOX (Figure 7b) can be caused by convective outflow. However, it can also be the consequence of the temperature dependence of the reaction of NO with O_3. Furthermore, the NO/NO_x ratio shows a secondary maximum in the mid troposphere between 4 and 5 km. The mean profiles of the tracers CO, CO_2, and O_3 measured during EULINOX do not show similarly large deviations in the upper troposphere. This supports the interpretation that the NO_x variability is caused at least partly by convective outflow and not by variations in the tropopause height.

3.2.   Mesoscale NO_x Signatures in Convective Clouds

[28]   In the last section we described NO_x enhancements found on the regional scale which could be attributed to cloud outflow from distant thunderstorms. Mixing with the ambient air slowly dilutes the NO_x plume. At this stage it is no longer possible to distinguish between the different NO_x sources (lightning and
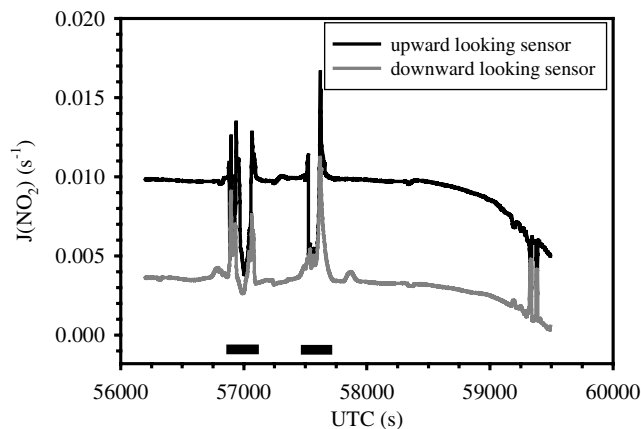
Figure 8. Photolysis frequencies $J(NO_2)$ versus time from the flight of 20 July (black line, upward looking sensor; gray line, downward looking sensor). During the penetration of two convective clouds (marked with the thick black lines), $J(NO_2)$ increased close to the cloud edges and decreased in the cloud centers. The decrease in $J(NO_2)$ after 58,500 s is caused by the decreasing flight altitude (descent for landing). Two small clouds were penetrated at about 59,300 s indicated by the short increase in the $J(NO_2)_{down}$ signal.

transport). In order to quantify the amount of NO_x produced by lightning we have to analyze single convective cloud events taking place more recently on the mesoscale instead of aged regional scale signatures.

3.2.1. Identification of convective cloud penetrations and estimate of average trace gas mixing ratios. [29] The times of cloud penetrations were roughly noted by the mission scientist on board the Falcon. Cloud penetrations can also be identified from

the measurements of vertical wind speed (which indicates well developed updrafts and downdrafts inside clouds), horizontal wind speed (changes distinctly in the cloud), CN concentration (which is smaller or larger inside clouds depending on washout processes), and $J(NO_2)$ photolysis frequency (which increases when approaching cloud edges and decreases inside clouds). To the best of our knowledge, the $J(NO_2)$ measurements are the first that have been performed extensively in thunderstorms. Such measurements have previously only been performed inside stratus and altocumulus clouds [*Kelley et al.*, 1995]. At the edges of convective clouds an increase in $J(NO_2)$ of up to 50% was registered due to light scattering by cloud particles (Figure 8). During some of the flights close to the cloud top region the upward looking $J(NO_2)$ sensor showed higher values than in the ambient air and distinctly higher values than the downward looking sensor. In the cloud center the upward and downward looking sensor showed similar photolysis frequencies. The intensity of sunlight was reduced, and $J(NO_2)$ decreased to half the values outside of the cloud (Figure 8). Model calculations by *Madronich* [1987] indicated an increase of 70% near cloud top and a decrease of 60% below cloud base in comparison to the ambient values. Similar ratios (range 1.7–2.3 and 0.4–0.9, respectively, of the ambient values) were observed by tethered-balloon measurements in low clouds by *Vilà-Guerau de Arellano et al.* [1994].

[30] For the EULINOX period, single convective cloud penetrations were selected by using the criteria mentioned above. Frequently, different criteria had to be used depending on the situation. Single convective cloud events were observed on the mesoscale on 3, 7, 14, 17, and 20 July; however, during most EULINOX flights it was not possible to penetrate the same convective cloud more than 1–2 times because of air traffic control restrictions. In all, 29 successful penetrations of convective clouds with and without lightning were found (cloud edge penetrations were not included, only penetrations straight through the clouds, mostly sideways). Although several convective clouds with a lot of lightning were penetrated also on 21 July, this day was excluded
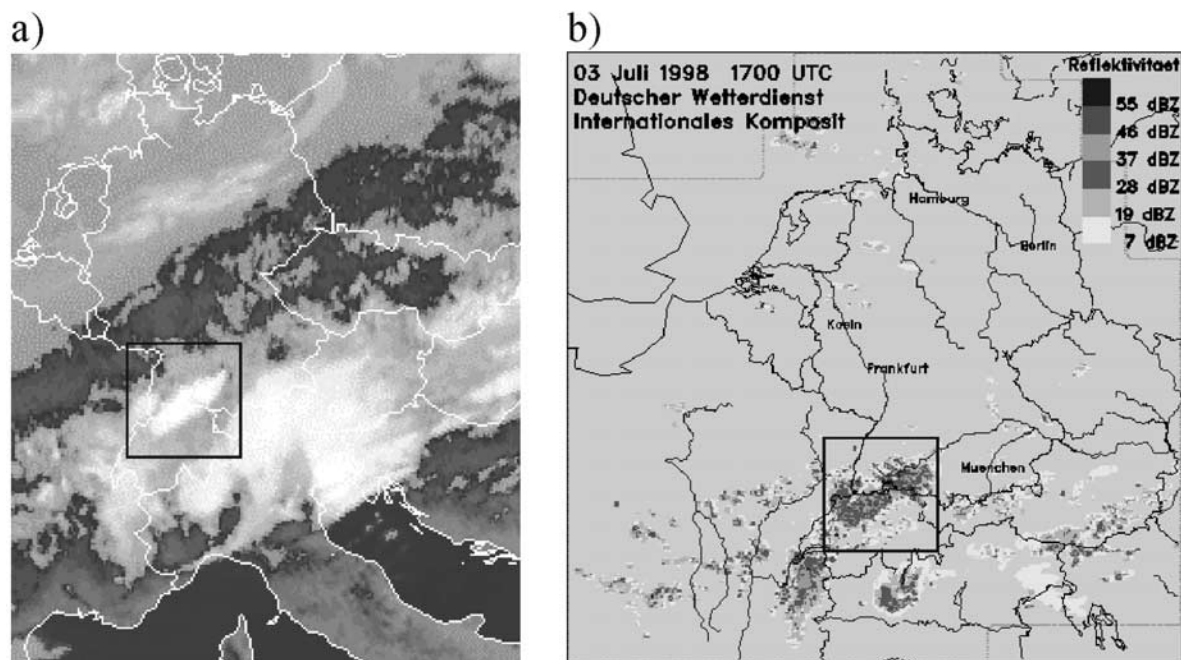

Figure 9. (a) METEOSAT-IR image for 1700 UTC 3 July. The black box indicates the investigated thunderstorms. (b) Radar image for 1700 UTC 3 July from the German Weather Service (DWD). Colors indicate different radar reflectivities (see legend). See color version of this figure at back of this issue.
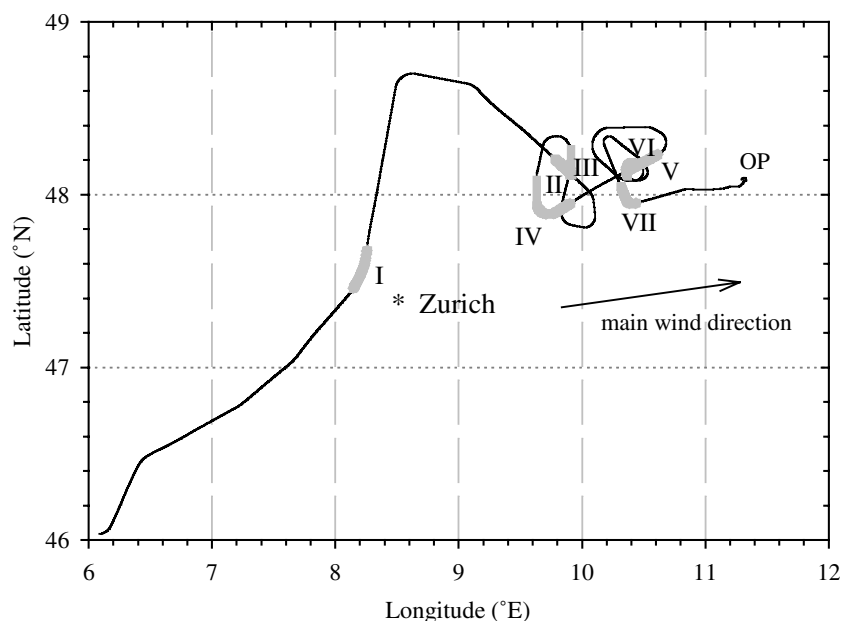
Figure 10. Map showing the flight track of the Falcon on 3 July (last part of the flight). Between Zurich and OP (Oberpfaffenhofen, operation site) a multicell storm system was penetrated. Penetrations of convective cells with (I and IV) and without lightning (II and III) are labeled. The convective outflow area ahead of the storm system is labeled V–VII.

from the study presented here. It is analyzed separately in section 3.3 because of the heavily polluted conditions in the PBL and the huge amount of observed NO spikes.

[31] In order to quantify the amount of NO_x produced by lightning in thunderclouds, different methods have been used [*Huntrieser et al.*, 1998; *Höller et al.*, 1999]. First of all, the amount of transported PBL NO_x to the anvil region has to be determined. The method described by *Höller et al.* [1999] and others requires complete vertical profiles of CO or CO_2 and NO_x down to the surface (the CO/ NO_x or CO_2/NO_x ratio in the PBL is used). A different approach was introduced by *Huntrieser et al.* [1998]. The mean CO_2 mixing ratio in convective clouds with lightning was very similar to the mixing ratio in nearby convective clouds without lightning. It can therefore be assumed that the amount of transported PBL NO_x is similar in both types of clouds and from this simple relationship the amount of lightning-produced NO_x in the anvil could be estimated. The method requires that mean trace gas concentrations are known. This was simply done by averaging all values observed during one cloud penetration (arithmetic mean). The analysis of single convective clouds without lightning during LINOX [*Huntrieser et al.*, 1998] showed similar mean NO_x concentrations ($\sim$0.5 ppbv) and only low standard deviations during these penetrations (0.1–0.2 ppbv). This result shows that the amount of PBL NO_x transported to the anvil region in thunderclouds is not very variable. In comparison, the mean NO_x mixing ratio calculated for different penetrations of thunderclouds was more variable, and the standard deviation in each case was almost half of the mean mixing ratio ($\sim$1.3 ppbv), which probably depend on the different lightning activity in the clouds (on how much NO_x is produced by lightning). In the next sections the method described above will be applied to the EULI-NOX data set.

3.2.2. Case 3 July 1998. [32] One typical day with several penetrations of convective clouds was 3 July. The black box in the METEOSAT-IR image and radar image (Figures 9a–9b) identifies the multicell storm system located at the border between Switzerland and Germany on that day. An enlargement of the last part of the flight track is presented in Figure 10. One convective cell with lightning (labeled I, 30 km in diameter) was

penetrated close to Zurich at 8 km altitude. Near Schaffhausen one cell almost without lightning was penetrated twice (labeled II and III, 15 km in diameter), and another cell with lightning was penetrated once (labeled IV, 40 km in diameter). Then the aircraft climbed (from 8 km) to the tropopause region ahead of the multicell storm system. The cloud-free outflow area, that reached at least 50 km ahead of the storm, was penetrated during the ascent (labeled V) and during the descent (labeled VI) between 8 and 10 km.

[33] Figures 11a–11b present trace gas signatures (NO, NO_x, CO_2, and CO) measured during the penetrations of the convective clouds at 8 km altitude (labeled I–IV) and in the cloud-free convective outflow areas (labeled V–VI). No O_3 data were available from this flight for the time period shown. At least seven distinct minima can be observed in CO_2 between 57,000 and 63,000 s. Six of the minima indicate concentrations down to 363 ppmv (labeled I–III and V–VII). In one minimum the concentration even dropped below 358 ppmv (labeled IV). The vertical CO_2 and CO ascent profiles from 3 July show very distinct differences between the PBL and the upper troposphere (Figures 12c–12d, cloud penetrations have been excluded) which can be used to identify PBL air convectively transported to the upper troposphere. The CO_2 minima and CO maxima measured in the clouds indicate clearly that the air has been transported from an altitude below 2.2 km according to the CO_2 and CO ascent profile. The vertical profiles were sampled ahead of the thunderstorm system (about 100 km) during the ascent in this case and are assumed to represent the trace gas concentrations in the thunderstorm inflow area.

[34] It is interesting to note that the lightning activity (CG flashes observed by the LPATS system) was quite variable in the different clouds investigated on 3 July, which may explain why clouds with about the same CO_2 minimum concentrations show very different NO concentrations (Figure 11a, I–IV). The first cloud penetration at 8 km (labeled I, around 58,000 s) was an intensive thunderstorm with high lightning frequency (22 CG flashes in 15 min) and NO mixing ratio (mean value 2 ppbv). The spiky NO structure (up to 6 ppbv) indicates that the NO increase was produced by very fresh lightning and the cell was
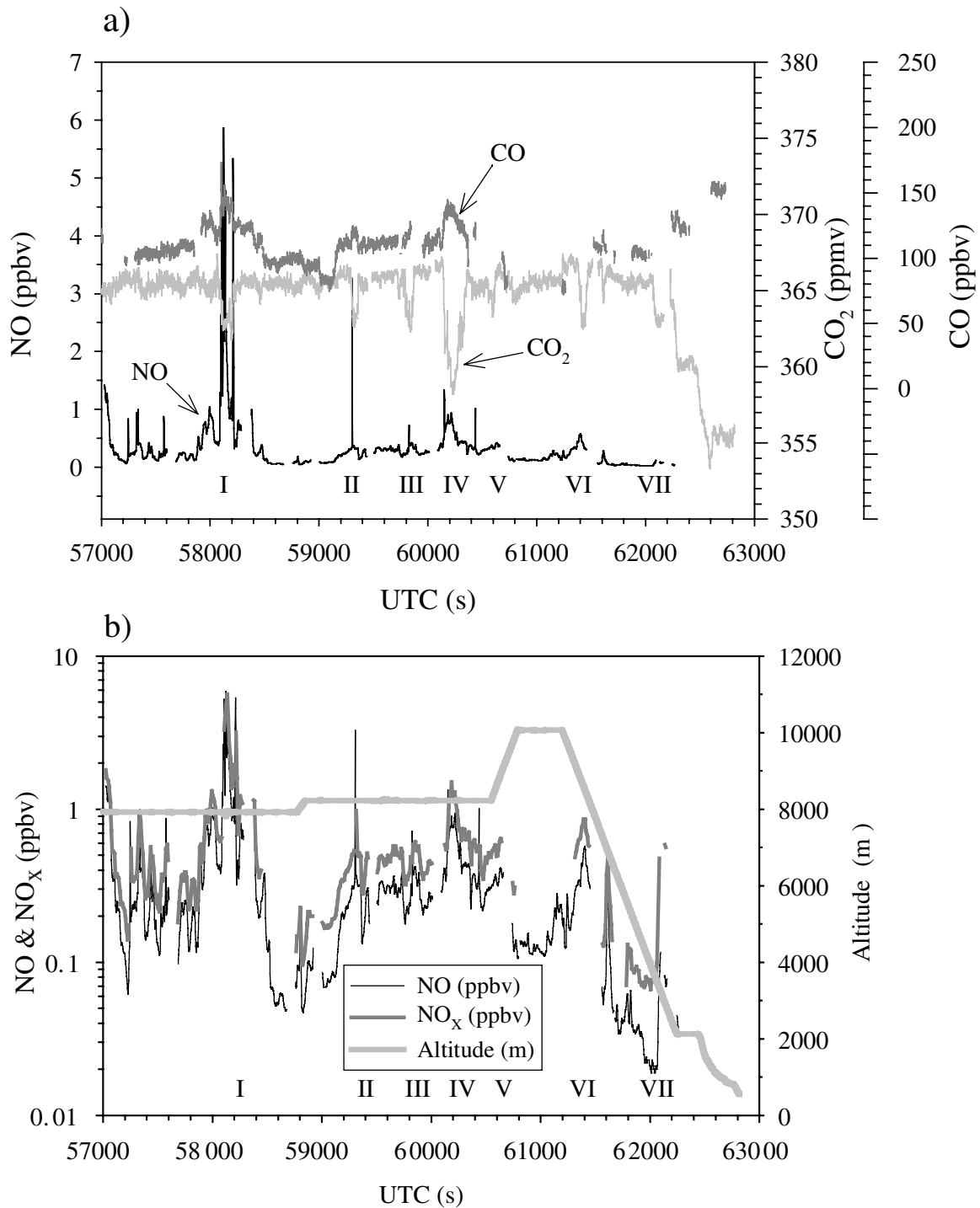
Figure 11. (a) Mixing ratio of NO (black line), CO_2 (light gray line), and CO (dark gray line) versus time from the flight of 3 July. Penetrations of four convective clouds with different lightning activity are labeled I–IV, and the cloud outflow area downwind of the storm line is labeled V–VII. (b) Mixing ratio of NO (thin black line), NO_x (dark gray line), and altitude (light gray line) versus time from the flight of 3 July.

penetrated close to the core. The second CO_2 minimum (II) close to 59,300 s shows a small NO enhancement with a single NO spike (3.3 ppbv) superimposed. This cloud had just started to be electrically active (1 flash in 15 min), and thus the NO observed in this cloud resulted mainly from transport from the PBL. The third CO_2 minimum (III) close to 59,800 s shows a small NO enhancement and a single small superimposed NO spike (0.7 ppbv). It is the same cloud that was penetrated just

before, and both penetrations were made sideways across the anvil. The mean NO concentration in this cloud (dominated by PBL air) was 0.3–0.4 ppbv (II–III penetration) and much lower than during the first cloud penetration. The fourth CO_2 minimum (IV) close to 60,200 s shows a rather distinct NO enhancement (mean value 0.6 ppbv) and at least one superimposed NO spike. Lightning was observed in this cloud several times during the last hour before the measurement
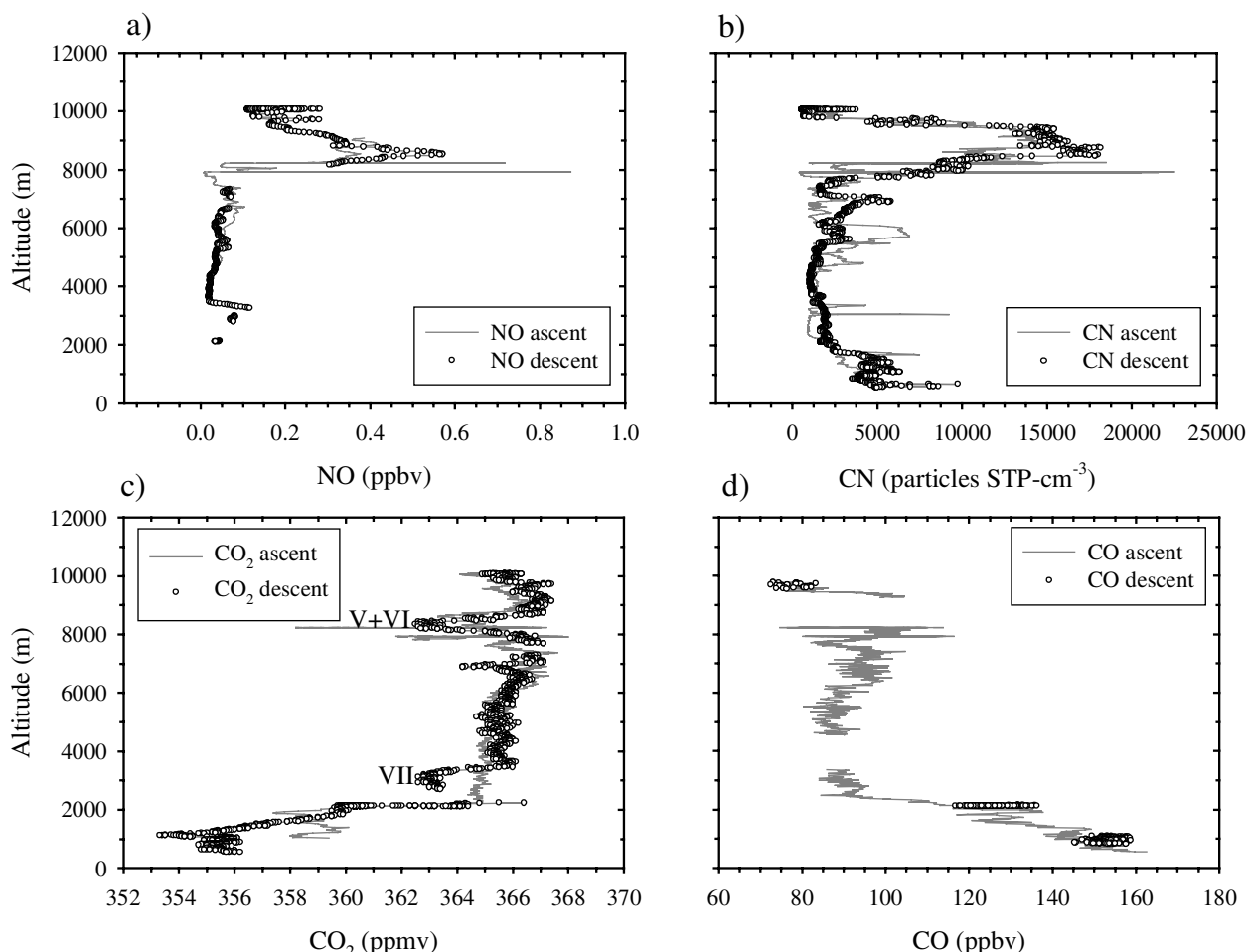
Figure 12. Concentrations of (a) NO, (b) CN, (c) CO_2, and (d) CO versus altitude for 3 July. The cloud outflow region in the upper troposphere is labeled V + VI, and the CO_2 decrease (NO increase) in the lower troposphere is labeled VII.

(3 flashes in 15 min) and caused the enhanced NO concentration together with transported NO from the PBL. This anvil was penetrated both along and sideways across.

[35] Some CO_2 minima were also found outside the investigated clouds. The clouds were organized along a line (Figures 9a–9b), and the CO_2 minima labeled V and VI, close to 60,600 and 61,400 s, were observed downwind of this line (close to II and III) in cloud-free air during the ascent and descent between 8 and 10 km. In the sections V and VI also high NO and CN values (Figures 12a–12b) were found between 8 and 9 km in a cloud-free area just below the tropopause (located at 9.7 km) similar to those described for the regional scale case. However, here the cloud outflow, coming from the west-southwest, was very fresh from nearby thunderstorms. The cloud outflow had a vertical extension of about 1 km, and the highest NO concentration (0.6 ppbv) and CN concentration (18,000 particles per STP cm^{-3}) were observed in the center of the cloud outflow area around 8.5 km altitude. The average NO_x concentration in the layer was 0.5 ppbv (Figure 7a). Both the NO_x and the CO_2 concentrations in the cloud-free outflow air are very similar to the ones observed inside clouds without lightning (II and III). This suggests that the cloud outflow mixed only slowly with the ambient air.

[36] The trace gas concentrations observed in clouds without lightning are used to estimate the amount of lightning-produced NO_x in clouds with lightning (Figure 13) since no NO_x/CO_2 ratio for PBL air was available. During the second and the third cloud penetration, almost no lightning was registered, and the average

NO_x enhancement of 0.5 ppbv can mainly be attributed to transport of polluted air from the PBL mixed with ambient air. The amount of lightning-produced NO_x in the first thunderstorm (I) can be estimated relative to the PBL NO_x observed in clouds II and III since we observed similar CO_2 concentrations during all three clouds penetrations originating from about the same altitude in the PBL. In the first thunderstorm (labeled I) an average NO_x concentration of 3.0 ppbv (due to lightning and PBL transport) was observed, while the PBL concentration was estimated to be at least 0.5 ppbv (assuming that there was no mixing with the ambient air). Hence we estimate that no more than 80% of the NO_x observed in this thunderstorm resulted from production by lightning and at least 20% resulted from the transport of PBL air. The same estimate was made for the fourth (IV) thunderstorm penetration. An average NO_x concentration of 0.9 ppbv was observed from which at least 60% resulted from transport from the PBL and no more than 40% resulted from production by lightning.

[37] The NO_x increase in the lower troposphere ahead of the storm (labeled VII), that was penetrated below 3.5 km before landing at OP, is also interesting to mention (Figures 11a and 12a). The mean concentrations measured for CO_2 (363 ppmv) and NO_x (0.5 ppbv) were similar to those measured before in the upper tropospheric cloud outflow. The minimum CO_2 concentration was also close to what was observed during the cloud penetrations (I, II–III) indicated in Figure 11a. The observed change in the lower tropospheric vertical profiles of NO_x and CO_2 is probably
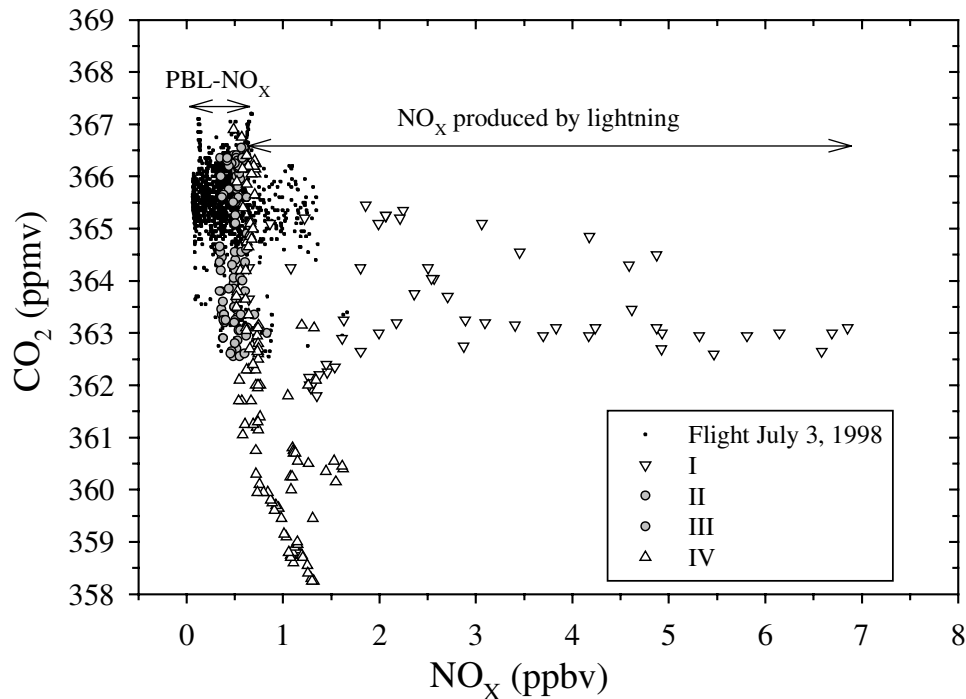
Figure 13. Data of CO_2 versus NO_x mixing ratios for the flight from 3 July. Convective clouds with lightning (labeled I + IV) and without lightning (labeled II + III) were penetrated. Arrows indicate the ranges of data obtained in clouds from transported PBL NO_x and from lightning-produced NO_x.

caused by the gustfront which spreads out cold downdraft air from midlevels of the storm in the lower PBL ahead of the storm. This cold air, which moves close to the surface, forces the warmer air ahead of the storm and the PBL to rise and a new inversion layer to develop at higher altitudes (3.5 km). Thus a second PBL top develops. A closer look at the case 1 July (section 3.1) shows also a CO_2 decrease (Figure 6c) and CN increase (Figure 6g) between 3 and 4 km indicating a similar behavior ahead of this thunderstorm system.

3.2.3.   Case 17 July 1998. [38] During two flights (17 and 21 July) the Falcon managed to follow a storm development over a longer time period and to penetrate each of these cloud systems seven times at different altitudes since we were flying in areas without heavy air traffic. On 17 July an isolated squall line near Bayrischer Wald in eastern Bavaria was investigated (30 × 60 km horizontal size). The squall line was in a dissipating stage and not very electrically active. We penetrated the squall line at three different altitudes. The observed NO and CO_2 mixing ratios are shown in Figure 14. Repeated penetrations at the same altitude showed similar average NO_x concentrations. The highest NO_x concentrations (horizontally) were found in the center of the anvil. At 7.6 km (cloud top) 0.9 ± 0.1 ppbv, at 7.3 km 1.4 ±
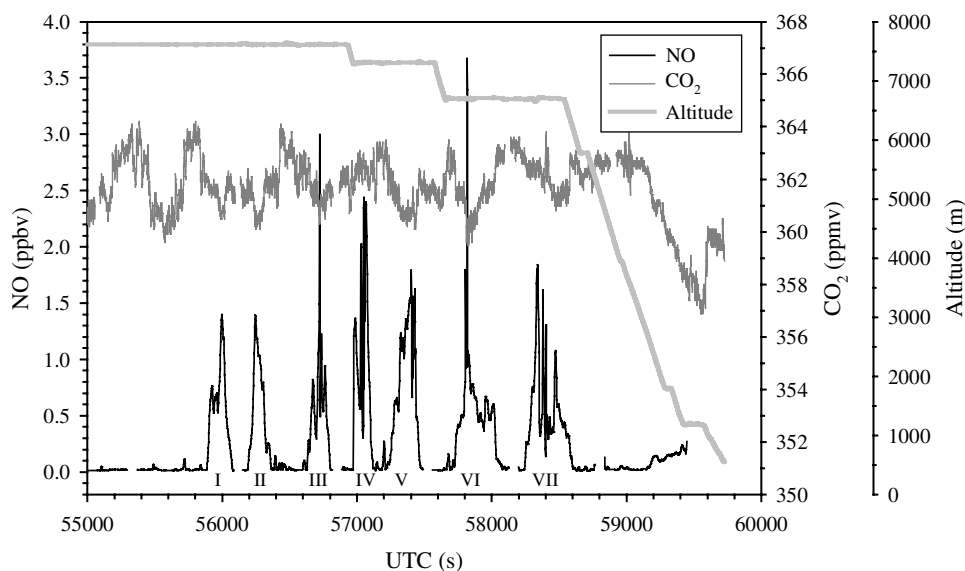

Figure 14. Mixing ratio of NO (black line) and CO_2 (dark gray line), and altitude (light gray line) versus time from the flight of 17 July. Seven penetrations of a squall line at different altitudes are labeled I–VII.

Table 3. Average NO_x Concentration in 29 Convective Clouds Observed During EULINOX

	Average NO_x in Convective Clouds Without Lightning, ppbv	Average NO_x in Convective Clouds With Lightning, ppbv
Minimum	0.2	0.5
Maximum	0.9	3.0
Mean plus or minus standard deviation	0.4 ± 0.2	1.3 ± 0.7

0.1 ppbv, and at 6.7 km 0.8 ± 0.1 ppbv, NO_x was measured. The related standard deviation was small for penetrations at the same altitude. The highest NO_x concentration was observed at 7.3 km. Here also the largest number of NO spikes were observed which indicates that this region was close to a region where lightning was generated (probably IC lightning; no measurements are available from the VHF interferometer for this area).

3.2.4. Amount of lightning-produced and transported NO_x in thunderstorms. [39] In section 3.2.2 it was shown that the air found in convective clouds without lightning seems to originate from the same altitude as air found in electrically active clouds. Such a comparison was not possible for every flight since the different types of electrically inactive and active clouds were not always found on the same day in the same area. Furthermore, the vertical CO_2 profile was not always as pronounced as described for the case of 3 July (10 ppmv difference between PBL and free troposphere). Therefore, in this section, we try to generalize our findings and estimate averages over all penetrated clouds of the same type. This is possible if the NO_x concentration at the top of the PBL does not change much (0.1–0.4 ppbv, Figure 7a), which is true for most days (except 21 July). It is very unlikely that the PBL was on average much more polluted in cases of electrically inactive clouds than in clouds with lightning.

[40] Single convective cloud events observed on the mesoscale during EULINOX on 3, 7, 14, 17, and 20 July will be studied next in detail. The analysis included 29 penetrations of convective clouds. The clouds were divided into two groups with (50%) and without (50%) lightning, and the average NO_x concentration in the upper 2 km cloud-anvil region was calculated for every cloud penetration (Table 3). The mean NO_x concentration in clouds without lightning (which is the mean of 15 average values), 0.4 ± 0.2 ppbv (same value as estimated for the top of the PBL), was used to estimate the ratio of transported and lightning-produced NO_x in clouds with lightning. For an average EULINOX thunderstorm (1.3 ± 0.7 ppbv NO_x), about 70% of the measured anvil NO_x was produced by lightning, and about 30% was transported PBL NO_x. In large EULINOX thunderstorms (average 3 ppbv NO_x) the amount of lightning-produced NO_x was found to exceed 80%. These values are close to the values inferred from the LINOX field experiment in 1996 where the same method to estimate the amount of lightning-produced NO_x was used [*Huntrieser et al.*, 1998]. Furthermore, these calculations again indicate that the air in convective clouds may originate from the top of the PBL. In the next section we will present another estimate that supports these findings.

3.2.5. Origin height of anvil air. [41] Mean trace gas concentrations in convective clouds without lightning were analyzed to investigate the origin height of anvil air and possible mixing processes. In the upper part of these clouds the mean NO_x, CO_2, and CO concentrations were 0.4 ± 0.2 ppbv, 362 ± 1 ppmv, and 115 ± 10 ppbv, respectively. By using the mean EULINOX profiles shown in Figures 6b, 6d, and 7a we can make a rough estimate from which altitude the air samples

observed in the cloud top regions originated. We have to assume that these profiles taken during the ascent and descent into OP are representative for the entire EULINOX investigation area where thunderstorms were found. According to CO_2, CO, and NO_x values the most probable origin height for the sampled air parcels (near cloud top) is 2 km (range 1.5–2.5 km) which is the top of the boundary layer (also observed by *Pickering et al.* [1988]). Trajectory analysis from a nonhydrostatic cloud model simulation of a STERAO thunderstorm by *Skamarock et al.* [2000] shows similar origin heights 0.5–2 km above the surface (our operation site is located almost 600 m above sea level). Upward transported air parcels during EULINOX seem to be like protective cores from the PBL with almost no mixing with the ambient air except in a narrow region near the cloud edges. Similar in situ observations were made by *Ström et al.* [1999] in cumulonimbus anvils over western Europe and by *Boe et al.* [1992] in thunderstorms over North Dakota. Model calculations by *Stenchikov et al.* [1996], *Prather and Jacob* [1997], *Cohan et al.* [1999], and *Skamarock et al.* [2000] also support our observations. However, recent calculations with an entraining/detraining convective plume model [*Mari et al.*, 2000] indicate that >50% of the anvil air originated above 6 km and not from the PBL (similar result as published by *Scala et al.* [1990]). Numerical simulations by *Wang and Crutzen* [1995] indicate that only a very small fraction of PBL air entered the anvil of a typical midlatitude storm (<10%). In contrast to the last mentioned model results, our measurements and calculations suggest that the fraction of PBL air dominates in the anvil (>50%) as indicated by the two most extreme possible cases from our observations: (1) origin height is top of the PBL (1.5 km above ground), and (2) origin height is 500 m above ground. In the first case, PBL air must be transported almost undiluted to agree with the observed mixing ratios in the clouds. In the second case, at least 50% PBL air must be mixed with less than 50% ambient air to agree with the observed mixing ratios in the clouds.

3.3. Microscale NO_x Signatures

3.3.1. Case of 21 July. [42] Microscale NO_x signatures (sharp NO spikes due to production by lightning) were observed frequently during the last EULINOX mission on 21 July. A very intensive, isolated thunderstorm developed in the evening west of Munich, marked in Figure 15a by a black box in the IR-METEOSAT image of 1800 UTC. The storm developed ahead of a larger cold front system extending from Scandinavia to Spain. Lightning activity was surveyed by the ONERA VHF mapper from 1400 until 2210 UTC [see also *Dotzek et al.*, 2000]. More than 12,000 flashes were reconstructed for this period of time. The cloud structure was also observed by radar and compared with a mesoscale model [*Höller et al.*, 2000].

[43] The Falcon penetrated the thundercloud seven times (passes 1–7) at different altitudes between 7 and 10 km very close to the operation site (distance 10–20 km). Figure 15b shows the most interesting part of the Falcon flight track and the registered 2-D density of the VHF signals (between 1740 and 1810 UTC). Time series of chemical and particle measurements for the entire flight are presented in Figures 16a and 16b. Between 1730 and 1845 UTC the isolated thunderstorm (diameter 40–50 km) described before was probed by the Falcon (starting at 63,500 s). The flight was exceptional because the Falcon passed close to the cell center below the anvil region. Inside the thunderstorm, lightning was observed by the aircraft crew several times. Very high NO peaks were measured. The highest NO mixing ratios (up to 25 ppbv) were measured during pass 3 of the storm (see Figure 16b). At the same time as one of these high NO spikes (24 ppbv) was observed (64,548 s), the aircraft nose was hit by a small lightning stroke shown in a video scene in Figure 17. The rear-facing sampling inlet for NO is located on the top of the Falcon about 5 m apart from the nose
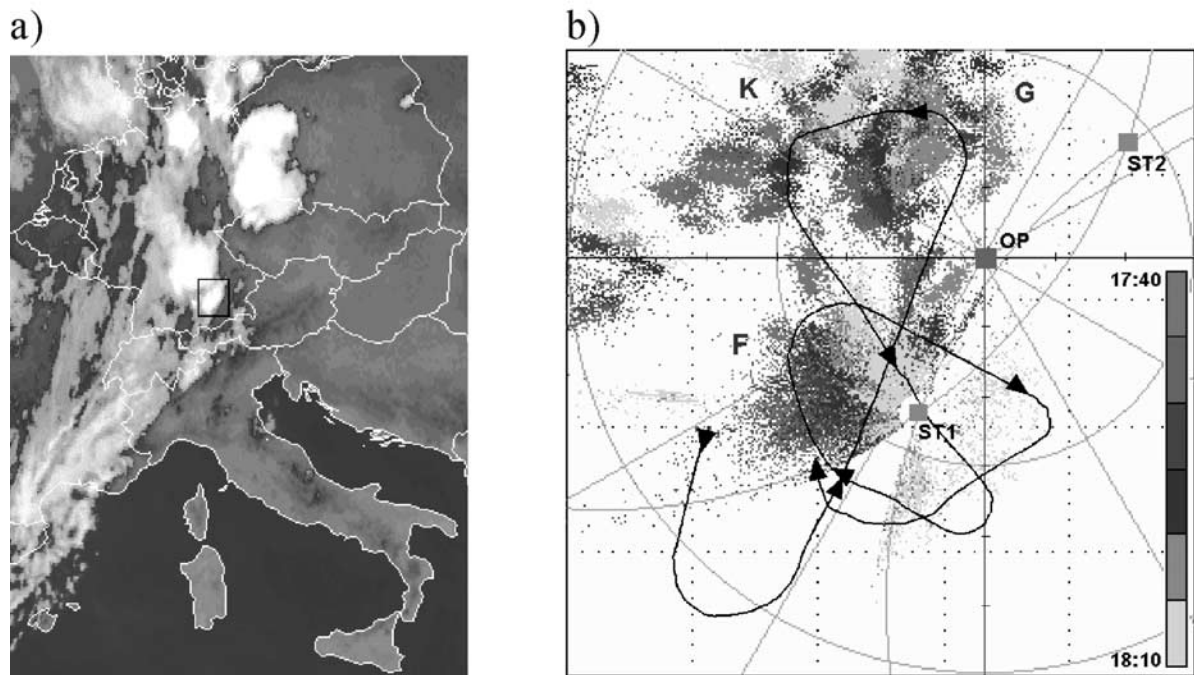
Figure 15. (a) METEOSAT-IR image of central Europe for 1800 UTC, 21 July. The thunderstorm investigated by the in situ measurements is marked by the black box. (b) Ground projection (90 × 90 km) of VHF sources detected by the ONERA system between 1740 and 1810 UTC, 21 July. Each color corresponds to a 5-min period. Red letters, labels of electrical cells; black line, Falcon trajectory during this time (1740−1810 UTC) with an arrow every 5 min; red squares, interferometric stations; blue square, operational center at Oberpfaffenhofen (48°N, 11°E). See color version of this figure at back of this issue.

boom. From the observations it cannot be told for sure that the NO spike was produced by this stoke; however, it can also not be excluded. A few minutes later during pass 5 the highest CN concentration peak was measured, reaching 35,000 particles STP cm^{-3} (see Figure 16a).

[44] Figure 18 shows the vertical profiles of CN and CO_2. In contrast to the vertical profiles presented earlier, the single convective cloud penetrations have not been excluded here. The vertical CO_2 profile was exceptional on 21 July with very high concentrations in the PBL (373 ppmv). Ahead of the approaching cold front, which triggered the thunderstorms in the evening, the wind was continuously from the east since the morning. Polluted air from Munich spread out over the area where the thunderstorm developed in the evening. The peak CO_2 mixing ratios observed at 8–10 km altitude inside the thunderstorm (Figure 18) were similar to those found in the PBL ahead of the thunderstorm. On 21 July both the Falcon and the DO-228 managed to characterize the inflow into the thunderstorm very well since the profiles were made just ahead of the thunderstorm. The observations indicate quick upward transport of polluted air from the PBL with little dilution by mixing, as also found by *Poulida et al.* [1996]. The chemical signatures found in the anvil region seem to partly "mirror" the polluted conditions at the top of the boundary layer (near 2.6 km this day) (also suggested by *Ström et al.* [1999]). The NO enhancement observed during the thunderstorm passes on 21 July was coincident with an enhancement in CO_2 (Figure 16a). The O_3 and CO_2 distribution in the PBL measured by the DO-228 shows relatively low variations in the thunderstorm inflow region with concentrations around 90 ± 10 ppbv and 368−372 ppmv, respectively (see Figures 6d and 6f). The enhanced O_3 mixing ratios in the boundary layer indicate that ozone smog conditions were predominant on 21 July.

3.3.2.   Estimate of lightning-produced NO. [45] The Falcon flight on 21 July was performed in a thunderstorm with

high lightning frequency (see Figure 15b). Fresh contributions from intracloud (IC) lightning can be expected in the upper part of the cloud (7–10 km). More than 150 NO spikes (Figure 16a) were registered during the thundercloud penetrations with widths between 0.3 and 2 km (mean 0.6 ± 0.4 km, median 0.4 km). The wider spikes were frequently composed of several narrow spikes (it was then impossible to separate individual spikes). The width of the spikes could also be less than 0.3 km, but this is the lower limit that can be detected with the highest resolution of the NO measurements (data available every 2 s since the 1 Hz data were averaged over 2 s). The dispersed hot lightning channel is probably far thinner, but the observed width may match the diameter of the corona sheath surrounding the lightning channel [*Zhang et al.*, 2000].

[46] The NO enhancement observed in the spikes (mean value 4.8 ppbv, median 2.9 ppbv) cannot only be attributed to the production by lightning, but also to convective transport from the polluted PBL. To distinguish between these two sources, CO_2 was used as tracer for PBL air. The CO_2 measurements were interrupted during the last part of the flight (Figure 16a). Therefore CO_2 data were only available for 92 of the observed NO spikes. It was searched for a correlation between NO_x and CO_2 to subtract the transported part of NO_x in the spikes. Because of the high humidity at lower altitudes on 21 July, the NO_x instruments were operated only above 5 km to avoid condensation on the cooled photomultiplier window. For this reason, no correlation between NO_x and CO_2 in the PBL is available for this day and therefore had to be constructed. An indication of the mean NO_x concentration in the PBL (mainly <1.2 ppbv) is available from other EULINOX mission days (Figure 7a). The transported part of NO was estimated from the data obtained during the single cloud penetrations on 21 July. From Figure 16a it can be seen that a spatially smooth NO enhancement (also visible in parts of the CO_2 signal) is superimposed by the spiky structure. Since this smooth NO
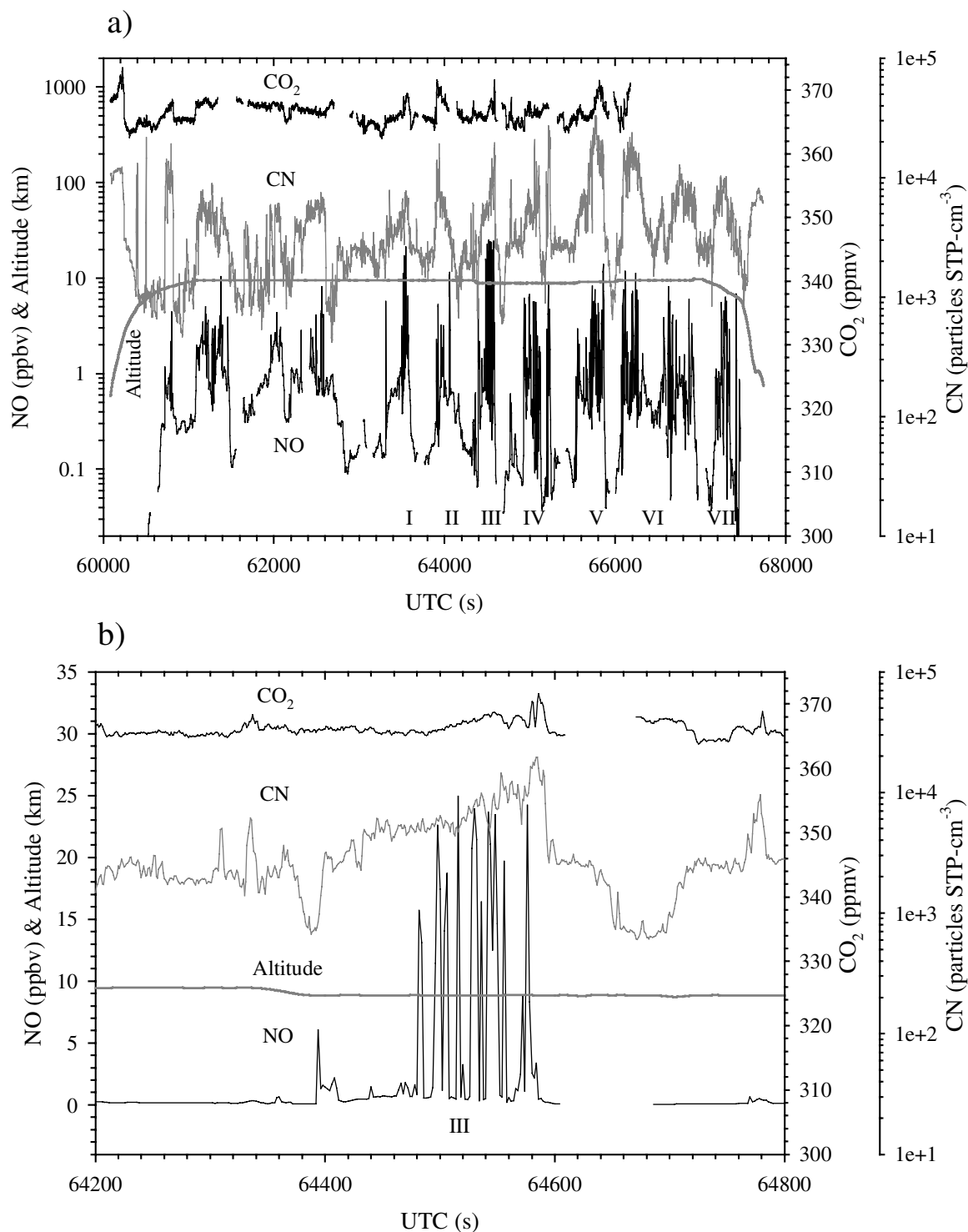
Figure 16.   Mixing ratios of NO and CO_2 and particle concentration (CN) versus time during the flight of 21 July. More than 100 NO spikes were observed. (a) The Falcon penetrated an isolated thunderstorm seven times after 63,500 s which is clearly visible in NO (labeled I–VII). (b) Penetration III is shown in detail.

enhancement roughly follows the CO_2 signal, it can be approximately attributed to that part of NO transported from the PBL. After cutting all NO spikes with values above 1.2 ppbv (as a first guess), a positive correlation between NO and CO_2 was found (Figure 19). For each CO_2 interval of 1 ppmv between 364 and 370 ppmv the average NO concentration and its standard deviation was calculated (Figure 19). The CO_2 axis points from high to low

values to reflect a profile of NO versus altitude. The strong increase in NO between 366.0 and 366.5 ppmv indicates that this is the transition zone between the conditions in the free troposphere and the PBL. This threshold is supported by the vertical CO_2 profile (see Figure 18), showing CO_2 values above 366 ppmv at and below the top of the PBL at 2.2 km. As a first attempt, the correlation between CO_2 and the mean NO value was used to

Figure 17. Video scene showing the lightning stroke which hit the Falcon meteorological boom at 1755:48 UTC on 21 July.

estimate the transported part of NO in the spikes. The calculated and the observed NO concentration (without spikes) was superimposed. It turned out that the calculated concentration was higher than the observed smooth NO signal (without spikes). The reason is probably that the average NO values in Figure 19 result from a mixture of transported PBL NO and aged lightning NO. Thus the lower limit of the measured NO values (mean value minus standard deviation) was used as a reasonable estimate for the transported NO part.

[47] If air from the PBL is characterized by a CO_2 concentration above 366.4 ppmv, then about 80% of the air in the upper part of the thunderstorm originated from the PBL. In the spikes the ratio was even higher with values around 90%. The correlation between NO and the tracer CO_2 was used to subtract the part of PBL NO in the spikes (≤ 0.6 ppbv). The residue (mean value 4.3 ppbv, median value 2.3 ppbv, range between 1 and 24 ppbv) was attributed to lightning. It is obvious that the NO contribution from the PBL (≤ 0.6 ppbv) is minor (10–20%) in comparison to the lightning-produced NO part (80–90%) in these spikes.

[48] We assumed that the NO contribution from the PBL was ≤ 0.6 ppbv on this day. From this value and the known NO/NO_x ratio (Figure 7b) the NO_x concentration that could have been
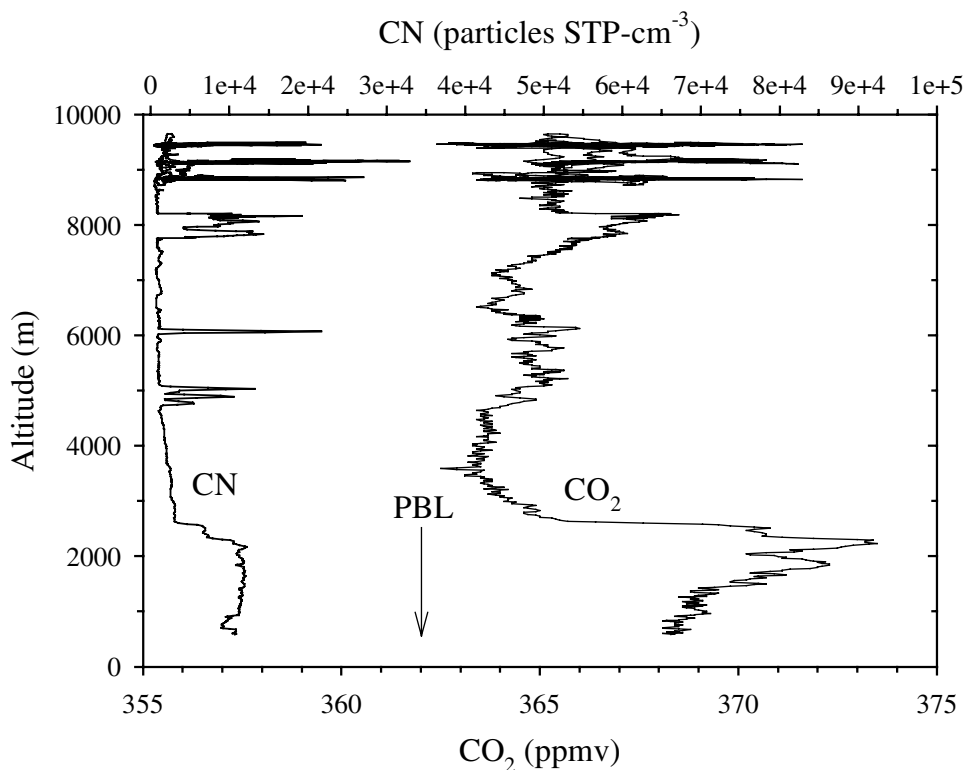

Figure 18. Vertical profile of CN (left) and CO_2 (right) as observed on 21 July. The planetary boundary layer (PBL) is discernible by high mixing ratios of CO_2 and a high CN concentration (below 2.6 km; ground at 0.6 km altitude).
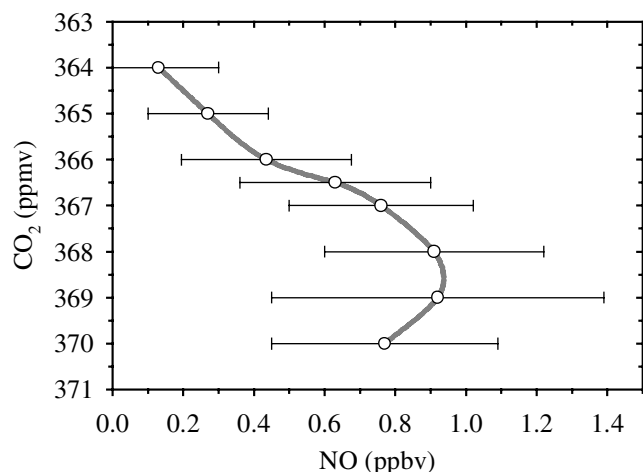
Figure 19. Mean value of NO versus CO_2 during the penetrations of the thunderstorm anvil on 21 July (labeled I–VI in Figure 16a). Note the reversed CO_2 axis. Horizontal bars indicate the standard deviation.

present in the upper half of the PBL this day (1.2 ppbv) was estimated. This NO_x concentration is distinctly higher than we can expect from the average conditions (0.4 ppbv NO_x; see Figure 7a). However, 21 July was an exceptional day with a very polluted PBL (Figure 18). Thus a 3 times higher NO_x concentration than on average seems reasonable. Figure 7a shows that an NO_x concentration of 1.2 ppbv in the PBL is within the range of the other EULINOX measurements.

3.3.3. Particle production. [49] The measurements within the thundercloud on 21 July showed not only large amounts of lightning-produced NO, but also a production of fine aerosol particles or condensation nuclei (CN) with diameters larger than 10 nm. CN concentrations up to 35,000 particles STP cm^{-3} were observed inside the thundercloud (see Figure 18), which is an exceptionally large value, even exceeding the particle concentration in the PBL. In order to quantify the amount of CN produced, the CO_2/CN relationship is plotted in Figure 20. Again, CO_2 concentration values above 366 ppmv serve as an indicator for PBL air. We considered only CN measurements above 8 km altitude at ambient temperatures between $-32°$ and $-42°C$ (to prevent misinterpretations of CN signals due to splitting supercooled droplets). The solid dots in Figure 20 identify cases with NO ≤ 0.6 ppbv (the limit deduced for PBL air, i.e., cases without contributions from lightning-produced NO_x). The open dots show cases with NO >0.6 ppbv (lightning-produced NO). The data are divided into one area with free troposphere (FT) signatures (CN < 5000 and CO_2 < 366 ppmv), one area with PBL signatures (CN < 12000, CO_2 > 366 ppmv), and one area with enhanced CN (CN > 12000, which is the maximum number of CN found in the PBL this day; see Figure 18). About 65% of the dots in the box "CN production" in Figure 20 show NO concentrations above 0.6 ppbv (all the open dots), which clearly indicates that CN particles are produced in regions where lightning enhances NO. Thus the major fraction of CN data points exceeding 12,000 particles STP cm^{-3} in Figure 20 are produced in the thunderstorm in air masses that also contain lightning-produced NO_x.

[50] These observations show that substantial amounts of new aerosol particles larger than 10 nm existed in the investigated air masses that evidently did not originate from upward transported PBL air. Recently, *Crawford et al.* [2000] also found high concentrations of ultrafine CN (<15 nm) in the convective outflow [see also *Jaeglé et al.*, 1998; *Liu et al.*, 1999; *Ström et al.*, 1999; *Thompson et al.*, 1999; *Koike et al.*, 2000]. However, the available information on aerosol microphysics does not allow us to identify with certainty the processes that could have led to the rapid
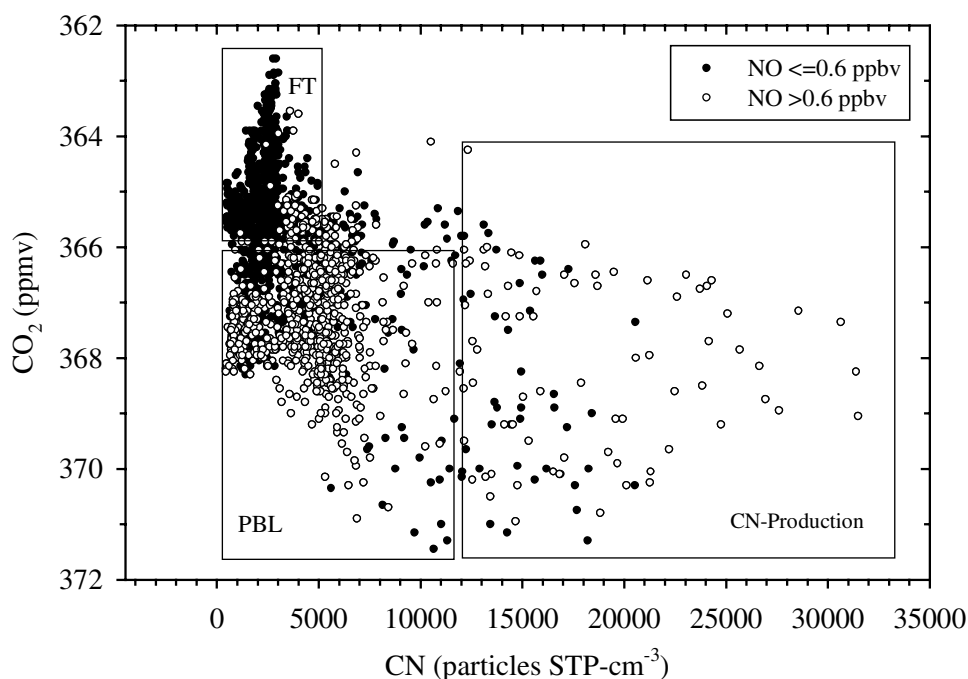

Figure 20. Mixing ratio of CO_2 versus concentration of CN observed inside and in the vicinity of the thundercloud investigated on 21 July. Solid dots represent data with NO mixing ratio below 0.6 ppbv (cases without lightning-produced NO), and open symbols are data with NO > 0.6 ppbv (with lightning-produced NO). Data areas with free troposphere (FT) signatures (CN < 5000 and CO_2 < 366 ppmv), with PBL signatures (CN < 12000, CO_2 > 366 ppmv), and with CN production signatures (CN > 12000) are indicated.

increase of detectable particles on 21 July. Possible processes include nucleation of new cluster-sized aerosols and enhanced condensation growth of initially undetectable small particles caused by rapid uplift, increased supersaturation and condensation of precursor species like H_2SO_4, H_2O, and possible condensable hydrocarbons [*Zhang et al.*, 1998; *Hendricks et al.*, 1999; *Laakso-nen et al.*, 2000]. The nucleation of new particles from condensable gases may be enhanced in clouds by washout of larger aerosols which otherwise would provide the surface for vapor deposition. High ion concentrations, possibly induced by the lightning, could also enhance the growth rate of molecular clusters [*Yu and Turco*, 2000].

4. Global and European Lightning NO_x Emission Rates

4.1. Estimate From Single Thunderstorm

[51] The results from single convective cloud penetrations (presented in Table 3; see also section 3.2.4) were used to estimate the global lightning NO_x production rate, $P(NO_x)$ [*Chameides et al.*, 1987]. The relation has also been used for the LINOX data analysis and is discussed in detail by *Huntrieser et al.* [1998].

$$P(NO_x) = [NO_x]F_C SC_1. \tag{1}$$

$[NO_x]$ is the average volume mixing ratio in the anvil produced by lightning, F_C is the average rate at which air is advected out of the anvil, S is the number of active cumulonimbus cells occurring at any instant globally, and C_1 is the conversion factor (1.5×10^7 g(N) g(air)$^{-1}$ s^{-1} yr^{-1}):

$$C_1 = \left(\frac{3600 \times 24 \times 365.25 \text{s}}{\text{year}}\right)\left[\frac{14\text{g(N)}}{\text{mole}}\right]\left[\frac{\text{mole}}{29\text{g(air)}}\right]. \tag{2}$$

The flux F_C of air mass out of the anvil can be estimated from

$$F_C = (v_a - v_s)\rho_a \Delta x \Delta z. \tag{3}$$

Here v_a is the horizontal wind speed inside the anvil, v_s is the velocity of the storm system (i.e., the wind speed at the steering level of the cloud, about one half of the ambient wind speed at the anvils altitude), ρ_a is the air density in the anvil, Δx is the width of the anvil, and Δz is the depth of the anvil. The mean values of these parameters during electrically active storms during EULINOX are $v_a - v_s = 7$ m s^{-1}, $\rho_a = 0.5$ kg m^{-3}, $\Delta x = 30$ km, $\Delta z = 1$ km, and $F_C = 1.1 \times 10^8$ kg s^{-1}. The air flux F_C is multiplied with the average NO_x concentration in the anvil due to production by lightning, which is 0.9 ppbv on average for all EULINOX cases, and the average number of thunderstorms occurring at any instant globally, which is about 2000 [*Brooks*, 1925; *Viemeister*, 1961]. From equations (1–3) we estimate that the global NO_x production rate due to lightning is about 3 Tg (N) yr^{-1}. The range of this estimate is about 1–20 Tg (N) yr^{-1} if we consider the variability of lightning NO_x and transported PBL NO_x in the anvil (Table 3). A similar mean value of 4 Tg (N) yr^{-1} was estimated from the previous field experiment LINOX [*Huntrieser et al.*, 1998]. The mean values estimated from the LINOX and EULINOX field experiments are slightly lower or equal to the frequently used mean values of 5 Tg (N) yr^{-1} [*Lee et al.*, 1997] and 4 Tg (N) yr^{-1} for the free troposphere only [*Bradshaw et al.*, 2000].

[52] We are aware of the fact that our measurements have only been performed in the midlatitudes over Europe and that these thunderstorms are perhaps not typical members of the global ensemble of thunderstorms. However, the flash frequency in European thunderstorms [*Finke and Hauf*, 1996] seems to be similar to the ones observed in midlatitude thunderstorms over the United States [*Orville*, 1994]. Maximum flash densities observed in the mountainous Black Forest in southern Germany ($\sim$10 yr^{-1} km^{-2}) were in the same order as values reported from Florida (9–13 yr^{-1} km^{-2}). However, the frequency of thunderstorms in Florida is twice as high as observed in southern Germany. Whether midlatitude thunderstorms are also similar to tropical storms is an open question. Furthermore, we assume that most of the NO_x in upper tropospheric penetrations of thunderstorms result from IC lightning (NO spikes). The amount of NO_x produced by CG lightning is probably not detected very well during these flights in the upper troposphere since some of this lightning-produced NO_x is transported downward with the downdraft. It is also very uncertain how much NO is produced by a CG flash in comparison to an IC flash [*Gallardo and Cooray*, 1996; *DeCaria et al.*, 2000; J. Bradshaw et al., unpublished manuscript, 1996]. Therefore 3 Tg (N) yr^{-1} estimated from EULINOX is probably a lower limit for the global NO_x production rate by lightning. The advantage of the method introduced by *Chameides et al.* [1987] is that $[NO_x]$ measured in the anvil is the sum of the production from all types of lightning flashes (no differentiation is necessary). On the other hand, it can sometimes be difficult to separate $[NO_x]$ measured in the anvil in lightning-produced and convective transported NO_x. In the next section a different method, which is based on NO spikes observed in thunderstorms, is presented to estimate the global lightning NO_x production rate.

4.2. Estimate From Observed NO Spikes

[53] The estimates of the lightning-produced part of NO in the spikes observed in the 21 July storm (section 3.3.2) can be used to calculate the production rate of NO molecules per m flash (as proposed by *Stith et al.* [1999] and others):

$$P_{NO} = \frac{PC[NO]\pi D^2}{4RT}, \tag{4}$$

where P is the pressure (Pa), C is the Avogadro constant (6.023×10^{23} molecules mol^{-1}), $[NO]$ is the NO volume mixing ratio, D is the diameter of the NO spike (m), R is the universal gas constant (8.314 J mol^{-1} K^{-1}), and T is the temperature (K). The residue of 2.3 ppbv (median value) which was attributed to lightning in the NO spikes (mean 4.3 ppbv, range between 1 and 24 ppbv) corresponds to a production rate of 2.7×10^{21} molecules NO per m flash (range $0.07 - 10 \times 10^{22}$). For comparison, *Stith et al.* [1999] reported similar but slightly smaller values (only 14 NO spikes were investigated: mean value 2.5×10^{21} and range $0.02 - 0.7 \times 10^{22}$ molecules NO per m flash).

[54] By using the median of the flash length (30 km) estimated during EULINOX (provided by ONERA [see *Höller and Schumann*, 2000]), the global flash rate of 65 s^{-1} [*Mackerras et al.*, 1998], and the median NO production rate found in this study (2.7×10^{21} molecules NO per m flash), it is estimated that on average 4 Tg(N) yr^{-1} (global value) result from lightning production if we assume that the investigated thunderstorm is a typical global thunderstorm. A similar value has been deduced from a model study by *Levy et al.* [1996] and a more recent laboratory study by *Wang et al.* [1998a]. In addition, *Bradshaw et al.* [2000, also unpublished manuscript, 1996] estimated the contribution of different kinds of flashes (IC, CG−, and CG+) to the global NO_x budget. Their result for NO_x production by IC lightning, 2.5 Tg(N) yr^{-1}, is close to our result.

[55] However, the combination of different flash lengths (5–50 km [see *Coppens et al.*, 1998; *Stith et al.*, 1999]), flash rates (40–120 s^{-1} [see *Turman and Edgar*, 1982; *Liaw et al.*, 1990; *Mackerras et al.*, 1998; *Christian et al.*, 1999]), and NO production rates (in this study $0.07 - 10 \times 10^{22}$ molecules NO per m flash) shows that the actual range can be very large (0.1–396 Tg(N) yr^{-1}) if we make estimates based on the NO production

Table 4. Summary of Estimates for NO_x Sources on the European and Global Scale

	Europe,[a] Tg(N) yr^{-1}	Global,[b] Tg(N) yr^{-1}
Fossil fuel combustion	6	22
Soils	1	7
Biomass burning	0.01	8
Lightning	0.03[c]	3[c]
Aircraft	0.1[d]	0.5

[a] *Simpson et al.* [1999].
[b] *Lee et al.* [1997] and *Bradshaw et al.* [2000].
[c] Estimates from EULINOX.
[d] D. Lee (personal communication, 1999).

per m flash. However, these values are the most extreme values possible, which may not be realistic, and the combination of the extremes may be unlikely. We also have to consider that the investigated NO spikes can contain NO from more than one flash. (In this study we assumed only one flash.) This implies a reduced NO production rate. At present, it is not possible to estimate how many flashes produced the NO observed in one spike. For such an investigation the sampling rate of the NO instrument must be changed from 1 s^{-1} to at least 10 s^{-1}.

[56] Furthermore, it was not possible to assign single NO spikes to single VHF signals because of the rather low spatial resolution of the VHF interferometer signals. For the 21 July thunderstorm these signals can only be estimated with an accuracy of about 1−2 km.

[57] All the uncertainties mentioned above show that the estimate of the global rate of lightning-produced NO_x from single NO spikes is very inaccurate. The global rate based on the NO_x outflow (mass flux) in single thunderstorms (section 4.1) appears to give the more reliable estimate of ∼3 Tg(N) yr^{-1}.

4.3. European and Global Lightning NO_x Emissions in Comparison to the Other NO_x Emissions

[58] The final step in the present study was to estimate the importance of European and global lightning NO_x emissions in comparison to the other NO_x emissions. The average European flash density (two flashes km^{-2} yr^{-1}) published recently by *Simpson et al.* [1999] is used to estimate the annual flash rate over Europe (0.7 flashes s^{-1}) and to compare it to the global flash rate (65 flashes s^{-1}). If the NO_x production rate by lightning scales with the flash rate, the European NO_x production rate by lightning is 1/100 of the global rate, which implies 0.03 Tg(N) yr^{-1} over Europe and 3 Tg(N) yr^{-1} globally, based on the value estimated from EULINOX. Table 4 lists the most important NO_x emissions on the European and global scale. On both scales the anthropogenic surface sources dominate clearly. However, in the upper troposphere, different sources dominate depending upon the investigated area. On the European scale, aircraft emissions dominate with 0.1 Tg(N) yr^{-1} (D. Lee, personal communication, 1999) in comparison to the production by lightning with 0.03 Tg(N) yr^{-1}. The opposite relationship can be found on the global scale, where lightning emissions dominate with 3 Tg(N) yr^{-1} in comparison to aircraft emissions with 0.6 Tg(N) yr^{-1}.

[59] In addition to the estimate of lightning-produced NO_x on the European scale, a rough estimate of the annual PBL NO_x mass flux due to thunderstorms can also be made. In the previous sections it was shown that on average about 30% of the anvil NO_x was transported PBL NO_x during EULINOX. Thus the annual amount of PBL-NO_x transported to the upper troposphere by single thunderstorms was estimated as 0.01 Tg(N) yr^{-1}, which is less than half of the NO_x amount produced by lightning in the upper troposphere and only about 1/10 of the aircraft-produced NO_x over Europe. We compared this number with the NO_x flux estimated

from the global mass flux from single thunderstorms (6.77×10^{18} kg PBL air per year) calculated by *Cotton et al.* [1995]. As described above, we use 1/100 of the global flux to achieve the flux for the European scale. In spite of the completely different method, the calculation gives again 0.01 Tg(N) yr^{-1} for the European PBL transport due to single thunderstorms. However, not only these types of thunderstorms transport NO_x from the PBL to the upper troposphere. We also have to consider the transport by larger mesoscale convective systems (MCS) and extratropical cyclones (mainly in the warm conveyor belt) which together transport globally about 6 times more air from the PBL than single thunderstorms [*Cotton et al.*, 1995]. If we assume the same relationship on the European scale (6 times higher mass flux), we end up with 0.08 Tg(N) yr^{-1} transported from the PBL by larger MCS and extratropical cyclones. Including the transport by single thunderstorms, we obtain almost 0.1 Tg(N) yr^{-1} for the European PBL transport, which is in the same range as the European emissions by aircraft and about 40% of the total NO_x in the upper troposphere over Europe. If we consider the total amount of NO_x emitted in the PBL over Europe (around 7 Tg(N) yr^{-1} in Table 4), about 1% of the PBL-NO_x is transported upward by convection and frontal systems. This result can be compared to simulations with a mesoscale chemical transport model (MCT) which were used to calculated the NO_x flux out of the PBL over Europe [*Hov and Flatøy*, 1997]. For the month July it was estimated that about 8% of the PBL NO_x emissions were transported to the free troposphere mainly by convection.

5. Summary and Conclusions

[60] The EULINOX field experiment was performed in the summer of 1998 over Europe. The present study analyzed the in situ observations in thunderstorms with the DLR research aircraft Falcon and DO-228 (equipped with chemical, particle, and meteorological instrumentation). In addition, lightning data from the European ATD, the German LPATS, and the VHF interferometer system of ONERA were used for interpretation of the airborne data.

[61] NO_x signatures observed on different atmospheric scales were analyzed to estimate the contribution of lightning-produced NO_x to the European and global nitrogen budget. NO_x enhancements were studied on regional scales over central Europe in thunderstorm clusters, on the mesoscale in convective clouds with and without lightning, and on the microscale in aged lightning channels. The highest NO_x concentrations were measured on the smallest scale. On 21 July several NO spikes with 25 ppbv were observed (the highest value ever reported for thundercloud anvils in the literature). The spiky NO signature in the thundercloud (on an average 20 spikes during each penetration) is probably the result of high lightning activity as observed with the VHF interferometer.

[62] High concentrations of particles (condensation nuclei (CN), size >10 nm) were also found in thunderstorm anvils. More complete CN measurements (number of small particles and composition) should be performed in the future to find out more about the origin of the particle production in thunderstorms. The CN may result from lightning and from transport of precursors from the PBL (e.g., SO_2, hydrocarbons, and chemiions), possibly favored by washout of larger aerosols. The large CN abundance observed in the thunderstorm outflow probably plays a significant role in the aerosol budget of the upper troposphere.

[63] During EULINOX, 29 convective cloud penetrations were analyzed in detail to estimate the origin of the NO_x enhancement found in all of the clouds. The strength of the NO_x increase in the clouds depends on the transport of polluted air masses from the PBL and on the production by lightning. In convective clouds without lightning, about 0.4 ppbv NO_x was observed to result from upward transport of polluted PBL air. In clouds with lightning the mean NO_x concentration reached 1.3 ppbv due to PBL transport and production by lightning. Tracers for PBL air, CO_2, and CO

were used to estimate the origin height of air masses found in the upper troposphere in these clouds. From the investigated tracers, CO_2 turned out to be the most useful one, mainly because of the more complete data set. The measured CO_2 vertical profile and the CO_2/NO_x correlation in clouds without lightning were used to estimate the amount of transported NO_x from the PBL in clouds with lightning. The convective air masses in the upper troposphere were found to originate mainly from a height close to the top of the PBL (about 1.5 km above the ground). On 21 July the PBL was extremely polluted, and this polluted air was transported upward very quickly by a thunderstorm that developed in the evening close to Munich. In the cloud outflow in the upper troposphere, trace gas concentrations were found which were similar to those in the polluted boundary layer. This example shows how effective thunderstorms are in redistributing trace gases in the troposphere. On average, about 70% of the NO_x enhancement measured in convective clouds with lightning was found to result from lightning, and about 30% was found to result from NO_x in the PBL. In clouds with high lightning frequency, lightning contributed to 90% of the measured NO_x increase. The high NO_x/NO_y ratio (exceeding 0.7) in these clouds indicates recent NO production by lightning.

[64] The global lightning NO_x production rate was estimated by using two different methods based on NO_x produced per thunderstorm [*Chameides et al.*, 1987] and NO produced per lightning flash [*Stith et al.*, 1999]. The median value for the production rate was estimated to 2.7 $\times$ 10^{21} molecules NO per m flash for EULINOX. In comparison to Stith et al., we went one step further and used this number to estimate the global lightning NO_x production rate (multiply it with global flash rate and flash length). However, the uncertainties in this estimate are huge (factor >100). The estimate derived from the NO_x outflow in single thunderstorms [after *Chameides et al.*, 1987] implies 3 Tg(N) yr^{-1} for the global lightning NO_x production rate based on the EULINOX data. This estimate also needs information on the global thunderstorm activity, which is not well known. Hence a range of 1–20 Tg(N) yr^{-1} for the global lightning NO_x production rate remains possible.

[65] One objective of this study was to compare the relative importance of NO_x produced by lightning and NO_x emitted by aircraft in the upper troposphere. On the global scale the effect of lightning production with 3 Tg(N) yr^{-1} is more important than aircraft emissions with 0.6 Tg(N) yr^{-1}. For the first time this relationship was also estimated on the European scale. Aircraft emissions dominate on the European scale with 0.1 Tg(N) yr^{-1} (D. Lee, personal communication, 1999), and the production by lightning is minor with 0.03 Tg (N) yr^{-1}. The estimated NO_x rate produced by lightning over Europe was compared to an independent calculation using OTD satellite data [*Nesbitt et al.*, 2000], which ends up with a rate of 0.026 Tg(N) yr^{-1} (S. W. Nesbitt and R. Zhang, personal communication, 2000). The agreement between both results is very good.

[66] A regional NO_x enhancement of order 0.5 ppbv, measured over central Europe on 1 July, could be traced back to a thunderstorm event farther upstream starting 1 day earlier. Such regional scale measurements could be used in the future to determine the various regional contributions to the NO_x budget by fitting the open source parameters in a regional CTM by optimally fitting the observations. For the future it is also recommended to conduct similar measurements in the tropics, where most lightning is observed and surface emissions of pollutants are generally small [*Benkovitz et al.*, 1996]. This could enhance the accuracy of estimates of global lightning-produced NO_x considerably.

References

Anderson, B. E., G. L. Gregory, J. E. Collins Jr., G. W. Sachse, T. J. Conway, and G. P. Whiting, Airborne observations of spatial and temporal variability of tropospheric carbon dioxide, *J. Geophys. Res.*, *101*, 1985–1997, 1996.

Bakwin, P. S., P. P. Tans, D. F. Hurst, and C. Zhao, Measurements of carbon dioxide on very tall towers: Results of the NOAA/CMDL program, *Tellus, Ser. B*, *50*, 401–415, 1998.

Beck, J. P., C. E. Reeves, F. A. A. M. de Leeuw, and S. A. Penkett, The effect of aircraft emissions on the tropospheric ozone in the northern hemisphere, *Atmos. Environ., Part A*, *26*, 17–29, 1992.

Beine, H. J., A. Dahlback, and J. B. Ørbæk, Measurements of $J(NO_2)$ at Ny-Ålesund, Svalbard, *J. Geophys. Res.*, *104*, 16,009–16,019, 1999.

Benkovitz, C. M., M. T. Scholtz, J. Pacyna, L. Tarrasón, J. Dignon, E. C. Voldner, P. A. Spiro, J. A. Logan, and T. E. Graedel, Global gridded inventories of anthropogenic emissions of sulfur and nitrogen, *J. Geophys. Res.*, *101*, 29,239–29,253, 1996.

Berntsen, T. K., and I. S. A. Isaksen, Effects of lightning and convection on changes in tropospheric ozone due to NO_x emissions from aircraft, *Tellus, Ser. B*, *51*, 766–788, 1999.

Boe, B. A., et al., The North Dakota Thunderstorm Project: A cooperative study of high plains thunderstorms, *Bull. Am. Meteorol. Soc.*, *73*, 145–160, 1992.

Bradshaw, J., D. Davis, G. Grodzinsky, S. Smyth, R. Newell, S. Sandholm, and S. Liu, Observed distributions of nitrogen oxides in the remote free troposphere from the NASA Global Tropospheric Experiment programs, *Rev. Geophys.*, *38*, 61–116, 2000.

Brasseur, G. P., J.-F. Müller, and C. Granier, Atmospheric impact of NO_x emissions by subsonic aircraft: A three-dimensional model study, *J. Geophys. Res.*, *101*, 1423–1428, 1996.

Brooks, C. E. P., The distribution of thunderstorms over the globe, *Geophys. Mem. London*, *3*, 147–164, 1925.

Brunner, D., J. Stähelin, and D. Jeker, Large-scale nitrogen oxide plumes in the tropopause region and implications for ozone, *Science*, *282*, 1305–1309, 1998.

Chameides, W. L., D. D. Davis, J. Bradshaw, M. Rodgers, S. Sandholm, and D. B. Bai, An estimate of the NO_x production rate in electrified clouds based on NO observations from the GTE/CITE 1 fall 1983 field operation, *J. Geophys. Res.*, *92*, 2153–2156, 1987.

Christian, H. J., et al., Global frequency and distribution of lightning as observed by the Optical Transient Detector (OTD), in *Proceedings of 11th International Conference on Atmospheric Electricity, Guntersville, Alabama*, pp. 726–729, 1999.

Clarke, A. D., J. L. Varner, F. Eisele, R. L. Mauldin, D. Tanner, and M. Litchy, Particle production in the remote marine atmosphere: Cloud outflow and subsidence during ACE 1, *J. Geophys. Res.*, *103*, 16,397–16,409, 1998.

Cohan, D. S., M. G. Schultz, D. J. Jacob, B. G. Heikes, and D. R. Blake, Convective injection and photochemical decay of peroxides in the tropical upper troposphere: Methyl iodide as a tracer of marine convection, *J. Geophys. Res.*, *104*, 5717–5724, 1999.

Coppens, F., R. Berton, A. Bondiou-Clergerie, and I. Gallimberti, Theoretical estimate of NO_x production in lightning corona, *J. Geophys. Res.*, *103*, 10,769–10,785, 1998.

Corbett, J. J., P. S. Fischbeck, and S. N. Pandis, Global nitrogen and sulfur inventories for oceangoing ships, *J. Geophys. Res.*, *104*, 3457–3470, 1999.

Cotton, W. R., G. D. Alexander, R. Hertenstein, R. L. Walko, R. L. McAnelly, and M. Nicholls, Cloud venting—A review and some new global annual estimated, *Earth Sci. Rev.*, *39*, 169–206, 1995.

Crawford, J., et al., Evolution and chemical consequences of lightning-produced NO_x observed in the North Atlantic upper troposphere, *J. Geophys. Res.*, *105*, 19,795–19,809, 2000.

Davis, D. D., et al., Assessment of ozone photochemistry in the western North Pacific as inferred from PEM-West A observations during fall 1991, *J. Geophys. Res.*, *101*, 2111–2134, 1996.

DeCaria, A. J., K. E. Pickering, G. L. Stenchikov, J. R. Scala, J. L. Stith, J. E. Dye, B. A. Ridley, and P. Laroche, A cloud-scale model study of lightning-generated NO_x in an individual thunderstorm during STER-AO-A, *J. Geophys. Res.*, 105, 11,601–11,616, 2000.

Defer, E., P. Blanchet, C. Théry, P. Laroche, J. Dye, M. Venticinque, and K. Cummins, Lightning activity for the July 10, 1996, storm during the STERAO-A experiment, *J. Geophys. Res.*, 106, 10,151–10,172, 2001.

Denning, A. S., D. A. Randall, G. J. Collatz, and P. J. Sellers, Simulations of terrestrial carbon metabolism and atmospheric CO_2 in a general circulation model, *Tellus, Ser. B*, 48, 543–567, 1996.

Dickerson, R. R., et al., Thunderstorms: An important mechanism in the transport of air pollutants, *Science*, 235, 460–465, 1987.

Dotzek, N., H. Höller, and C. Théry, Lightning and microphysics in a EULINOX supercell storm, *Phys. Chem. Earth B*, 25, 1285–1288, 2000.

Dye, J. E., et al., An overview of the Stratospheric-Tropospheric Experiment: Radiation, Aerosols, and Ozone (STERAO)-Deep convection experiment with results for the July 10, 1996, storm, *J. Geophys. Res.*, 105, 10,023–10,045, 2000.

Ehhalt, D. H., F. Rohrer, and A. Wahner, Sources and distribution of NO_x in the upper troposphere at northern midlatitudes, *J. Geophys. Res.*, 97, 3725–3738, 1992.

Feigl, C., Aufbau und Charakterisierung eines Meßsystems für NO, NO_2 und NO_y: Laboruntersuchungen und Einsatz in der unteren arktischen Stratosphäre, Ph.D. thesis, Deutsche Luft- und Raumfahrt Oberpfaffenhofen, Wessling, Germany, 1998.

Finke, U., and T. Hauf, The characteristics of lightning occurrence in southern Germany, *Contrib. Atmos. Phys.*, 69, 361–374, 1996.

Flatøy, F., and Ø. Hov, NO_x from lightning and the calculated chemical composition of the free troposphere, *J. Geophys. Res.*, 102, 21,373–21,381, 1997.

Flatøy, F., A. G. Kraabøl, and Ø. Hov, Regional model simulations and development of lightning NO_x emissions inventories, in *EULINOX — The European Lightning Nitrogen Oxides Project*, edited by H. Höller and U. Schumann, *Rep. DLR-FB—2000-28*, pp. 179–192, Deutsche Luft- und Raumfahrt Oberpfaffenhofen, Wessling, Germany, 2000.

Gallardo, L., and V. Cooray, Could cloud-to-cloud discharges be as effective as cloud-to-ground discharges in producing NO_x?, *Tellus, Ser. B*, 48, 641–651, 1996.

Gerbig, C., D. Kley, A. Volz-Thomas, J. Kent, K. Dewey, and D. S. McKenna, Fast-response resonance fluorescence CO measurements aboard the C-130: Instrument characterization and measurements made during NARE '93, *J. Geophys. Res.*, 101, 29,229–29,238, 1996.

Gerbig, C., S. Schmitgen, D. Kley, A. Volz-Thomas, K. Dewey, and D. Haaks, An improved fast-response vacuum-UV resonance fluorescence CO instrument, *J. Geophys. Res.*, 104, 1699–1704, 1999.

Grewe, V., D. Brunner, M. Dameris, J. L. Grenfell, R. Hein, D. Shindell, and J. Stähelin, Origin and variability of upper tropospheric nitrogen oxides and ozone at northern mid-latitudes, *Atmos. Environ.*, 35, 3421–3433, 2001.

Hagen, M., B. Bartenschlager, and U. Finke, Motion characteristics of thunderstorms in southern Germany, *Meteorol. Appl.*, 6, 227–239, 1999.

Hannan, J. R., et al., Atmospheric chemical transport based on high-resolution model-derived winds: A case study, *J. Geophys. Res.*, 105, 3807–3820, 2000.

Hauf, T., P. Schulte, R. Alheit, and H. Schlager, Rapid vertical trace gas transport by an isolated midlatitude thunderstorm, *J. Geophys. Res.*, 100, 22,957–22,970, 1995.

Hendricks, J., E. Lippert, H. Petry, and A. Ebel, Heterogeneous reactions on and in sulfate aerosols: Implications for the chemistry of the midlatitude tropopause region, *J. Geophys. Res.*, 104, 5531–5550, 1999.

Höller, H., and U. Schumann (Eds.), EULINOX—The European Lightning Nitrogen Oxides Project, *Rep. DLR-FB 2000-28*, 240 pp., Deutsche Luft- und Raumfahrt Oberpfaffenhofen, Wessling, Germany, 2000.

Höller, H., V. N. Bringi, J. Hubbert, M. Hagen, and P. F. Meischner, Life cycle and precipitation formation in a hybrid-type hailstorm revealed by polarimetric and Doppler radar measurements, *J. Atmos. Sci.*, 51, 2500–2522, 1994.

Höller, H., U. Finke, H. Huntrieser, M. Hagen, and C. Feigl, Lightning-Produced NO_x (LINOX): Experimental design and case study results, *J. Geophys. Res.*, 104, 13,911–13,922, 1999.

Höller, H., T. Fehr, C. Théry, J. Seltmann, and H. Huntrieser, Radar, lightning, airborne observations and modeling of a supercell storm during EULINOX, *Phys. Chem. Earth B*, 25, 1281–1284, 2000.

Hov, Ø., and F. Flatøy, Convective redistribution of ozone and oxides of nitrogen in the troposphere over Europe in summer and fall, *J. Atmos. Chem.*, 28, 319–337, 1997.

Huntrieser, H., H. Schlager, P. van Velthoven, P. Schulte, H. Ziereis, U. Schumann, F. Arnold, and J. Ovarlez, In-situ trace gas observations in dissipating thunderclouds during POLINAT, paper presented at 12th International Conference on Clouds and Precipitation, Int. Assoc. of Meteorol. and Atmos. Sci., Zurich, Switzerland, 1996.

Huntrieser, H., H. Schlager, C. Feigl, and H. Höller, Transport and production of NO_x in electrified thunderstorms: Survey of previous studies and new observations at midlatitudes, *J. Geophys. Res.*, 103, 28,247–28,264, 1998.

Intergovernmental Panel on Climate Change (IPCC), *Aviation and the Global Atmosphere,* edited by J. E. Penner et al., 373 pp., Cambridge Univ. Press, New York, 1999.

Jaeglé, L., D. J. Jacob, Y. Wang, A. J. Weinheimer, B. A. Ridley, T. L. Campos, G. W. Sachse, and D. E. Hagen, Sources and chemistry of NO_x in the upper troposphere over the United States, *Geophys. Res. Lett.*, 25, 1705–1708, 1998.

Jaeglé, L., et al., Ozone production in the upper troposphere and the influence of aircraft during SONEX: Approach of NO_x-saturated conditions, *Geophys. Res. Lett.*, 26, 3081–3084, 1999.

Jeker, D. P., L. Pfister, A. M. Thompson, D. Brunner, D. J. Boccippio, K. E. Pickering, H. Wernli, Y. Kondo, and J. Stähelin, Measurements of nitrogen oxides at the tropopause: Attribution to convection and correlation with lightning, *J. Geophys. Res.*, 105, 3679–3700, 2000.

Kelley, P., R. R. Dickerson, W. T. Luke, and G. L. Kok, Rate of NO_2 photolysis from the surface to 7.6 km altitude in clear sky and clouds, *Geophys. Res. Lett.*, 22, 2621–2624, 1995.

Koike, M., et al, Impact of aircraft emissions on reactive nitrogen over the North Atlantic flight corridor region, *J. Geophys. Res.*, 105, 3665–3677, 2000.

Laaksonen, A., et al., Upper tropospheric SO_2 conversion into sulfuric acid aerosols and cloud condensation nuclei, *J. Geophys. Res.*, 105, 1459–1469, 2000.

Lamarque, J.-F., G. P. Brasseur, P. G. Hess, and J.-F. Müller, Three-dimensional study of the relative contributions of the different nitrogen sources in the troposphere, *J. Geophys. Res.*, 101, 22,955–22,968, 1996.

Lee, D. S., I. Köhler, E. Grobler, F. Rohrer, R. Sausen, L. Gallardo-Klenner, J. G. J. Olivier, F. J. Dentener, and A. F. Bouwman, Estimations of global NO_x emissions and their uncertainties, *Atmos. Environ.*, 31, 1735–1749, 1997.

Lelieveld, J., and F. J. Dentener, What controls tropospheric ozone?, *J. Geophys. Res.*, 105, 3531–3551, 2000.

Levy, H., II, W. J. Moxim, and P. S. Kasibhatla, A global three-dimensional time-dependent lightning source of tropospheric NO_x, *J. Geophys. Res.*, 101, 22,911–22,922, 1996.

Liaw, Y. P., D. L. Sisterson, and N. L. Miller, Comparison of field, laboratory, and theoretical estimates of global nitrogen fixation by lightning, *J. Geophys. Res.*, 95, 22,489–22,494, 1990.

Liu, S. C., Possible effects on tropospheric O_3 and OH due to NO emissions, *Geophys. Res. Lett.*, 4, 325–328, 1977.

Liu, S. C., et al., Sources of reactive nitrogen in the upper troposphere during SONEX, *Geophys. Res. Lett.*, 26, 2441–2444, 1999.

Logan, J. A., Nitrogen oxides in the troposphere: Global and regional budgets, *J. Geophys. Res.*, 88, 10,785–10,807, 1983.

Luke, W. T., R. R. Dickerson, W. F. Ryan, K. E. Pickering, and L. J. Nunnermacker, Tropospheric chemistry over the lower Great Plains of the United States, 2, Trace gas profiles and distributions, *J. Geophys. Res.*, 97, 20,647–20,670, 1992.

Mackerras, D., M. Darveniza, R. E. Orville, E .R. Williams, and S. J. Goodman, Global lightning: Total, cloud, and ground flash estimates, *J. Geophys. Res.*, 103, 19,791–19,809, 1998.

Madronich, S., Photodissociation in the atmosphere, 1, Actinic flux and the effects of ground reflections and clouds, *J. Geophys. Res.*, 92, 9740–9752, 1987.

Mari, C., D. J. Jacob, and P. Bechtold, Transport and scavenging of soluble gases in a deep convective cloud, *J. Geophys. Res.*, 105, 22,255–22,267, 2000.

Michalon, N., A. Nassif, T. Saouri, J. F. Royer, and C. A. Pontikis, Contribution to the climatological study of lightning, *Geophys. Res. Lett.*, 26, 3097–3100, 1999.

Nesbitt, S. W., R. Zhang, and R. E. Orville, Seasonal and global NO_x production by lightning estimated from the Optical Transient Detector (OTD), *Tellus, Ser. B*, 52, 1206–1215, 2000.

Orville, R. E., Cloud-to-ground lightning flash characteristics in the contiguous United States: 1989–1991, *J. Geophys. Res.*, 99, 10,833–10,841, 1994.

Pickering, K. E., R. R. Dickerson, G. J. Huffman, J. F. Boatman, and A. Schanot, Trace gas transport in the vicinity of frontal convective clouds, *J. Geophys. Res.*, 93, 759–773, 1988.

Pickering, K. E., A. M. Thompson, W.-K. Tao, and T. L. Kucsera, Upper tropospheric ozone production following mesoscale convection during STEP/EMEX, *J. Geophys. Res.*, 98, 8737–8749, 1993.

Pickering, K. E., et al., Convective transport of biomass burning emissions

over Brazil during TRACE-A, *J. Geophys. Res.*, *101*, 23,993–24,012, 1996.

Poulida, O., R. R. Dickerson, and A. Heymsfield, Stratosphere-troposphere exchange in a midlatitude mesoscale convective complex, 1, Observations, *J. Geophys. Res.*, *101*, 6823–6836, 1996.

Prather, M. J., and D. J. Jacob, A persistent imbalance in HO_x and NO_x photochemistry of the upper troposphere driven by deep tropical convection, *Geophys. Res. Lett.*, *24*, 3189–3192, 1997.

Price, C., J. Penner, and M. Prather, NO_x from lightning, 1, Global distribution based on lightning physics, *J. Geophys. Res.*, *102*, 5929–5941, 1997.

Reeve, N., and R. Toumi, Lightning activity as an indicator of climate change, *Q. J. R. Meteorol. Soc.*, *125*, 893–903, 1999.

Ridley, B. A., M. A. Carroll, and G. L. Gregory, Measurements of nitric oxide in the boundary layer and free troposphere over the Pacific Ocean, *J. Geophys. Res.*, *92*, 2025–2047, 1987.

Ridley, B. A., J. E. Dye, J. G. Walega, J. Zheng, F. E. Grahek, and W. Rison, On the production of active nitrogen by thunderstorms over New Mexico, *J. Geophys. Res.*, *101*, 20,985–21,005, 1996.

Scala, J. R., et al., Cloud draft structure and trace gas transport, *J. Geophys. Res.*, *95*, 17,015–17,030, 1990.

Schlager, H., P. Konopka, P. Schulte, U. Schumann, H. Ziereis, F. Arnold, M. Klemm, D. E. Hagen, P. D. Whitefield, and J. Ovarlez, In situ observations of air traffic emission signatures in the North Atlantic flight corridor, *J. Geophys. Res.*, *102*, 10,739–10,750, 1997.

Schröder, F. P., B. Kärcher, A. Petzold, R. Baumann, R. Busen, C. Höll, and U. Schumann, Ultrafine aerosol particles in aircraft plumes: In situ observations, *Geophys. Res. Lett.*, *25*, 2789–2792, 1998.

Schulte, P., H. Schlager, H. Ziereis, U. Schumann, S. L. Baughum, and F. Deidewig, NO_x emissions indices of subsonic long-range jet aircraft at cruise altitude: In situ measurements and predictions, *J. Geophys. Res.*, *102*, 21,431–21,442, 1997.

Schumann, U., P. Konopka, R. Baumann, R. Busen, T. Gerz, H. Schlager, P. Schulte, and H. Volkert, Estimate of diffusion parameters of aircraft exhaust plumes near the tropopause from nitric oxide and turbulence measurements, *J. Geophys. Res.*, *100*, 14,147–14,162, 1995.

Schumann, U., H. Schlager, F. Arnold, J. Ovarlez, H. Kelder, Ø. Hov, G. Hayman, I. S. A. Isaksen, J. Stähelin, and P. D. Whitefield, Pollution from aircraft emissions in the North Atlantic flight corridor: Overview on the POLINAT project, *J. Geophys. Res.*, *105*, 3605–3631, 2000.

Shetter, R. E., and M. Müller, Photolysis frequency measurements using actinic flux spectroradiometry during the PEM-Tropics mission: Instrumentation description and some results, *J. Geophys. Res.*, *104*, 5647–5661, 1999.

Simpson, D., et al., Inventorying emissions from nature in Europe, *J. Geophys. Res.*, *104*, 8113–8152, 1999.

Skamarock, W. C., J. G. Powers, M. Barth, J. E. Dye, T. Matejka, D. Bartels, K. Baumann, J. Stith, D. D. Parrish, and G. Hübler, Numerical simulation of the 10 July Stratospheric-Tropospheric Experiment: Radiation, Aerosols, and Ozone/Deep convection experiment convective system: Kinematics and transport, *J. Geophys. Res.*, *105*, 19,973–19,990, 2000.

Smyth, S. B., et al., Factors influencing the upper free tropospheric distribution of reactive nitrogen over the South Atlantic during the TRACE-A experiment, *J. Geophys. Res.*, *101*, 24,165–24,186, 1996.

Solomon, R., and M. Baker, Lightning flash rate and type in convective storms, *J. Geophys. Res.*, *103*, 14,041–14,057, 1998.

Stenchikov, G., R. Dickerson, K. Pickering, W. Ellis, Jr., B. Doddridge, S. Kondragunta, O. Poulida, J. Scala, and W.-K. Tao, Stratosphere-troposphere exchange in a midlatitude mesoscale convective complex, 2, Numerical simulations, *J. Geophys. Res.*, *101*, 6837–6851, 1996.

Stith, J., J. Dye, B. Ridley, P. Laroche, E. Defer, K. Baumann, G. Hübler, R. Zerr, and M. Venticinque, NO signatures from lightning flashes, *J. Geophys. Res.*, *104*, 16,081–16,089, 1999.

Stockwell, D. Z., C. Giannakopoulos, P.-H. Plantevin, G. D. Carver, M. P. Chipperfield, K. S. Law, J. A. Pyle, D. E. Shallcross, and K.-Y. Wang, Modeling NO_x from lightning and its impact on global chemical fields, *Atmos. Environ.*, *33*, 4477–4493, 1999.

Ström, J., H. Fischer, J. Lelieveld, and F. Schröder, In situ measurements of

microphysical properties and trace gases in two cumulonimbus anvils over western Europe, *J. Geophys. Res.*, *104*, 12,221–12,226, 1999.

Thompson, A. M., L. C. Sparling, Y. Kondo, B. E. Anderson, G. L. Gregory, and G. W. Sachse, Perspectives on NO, NO_y, and fine aerosol sources and variability during SONEX, *Geophys. Res. Lett.*, *26*, 3073–3076, 1999.

Turman, B. N., and B. C. Edgar, Global lightning distributions at dawn and dusk, *J. Geophys. Res.*, *87*, 1191–1206, 1982.

Viemeister, P. E., *The Lightning Book*, Doubleday, New York, 1961.

Vilà-Guerau de Arellano, J., P. G. Duynkerke, and M. van Weele, Tethered-balloon measurements of actinic flux in a cloud-capped marine boundary layer, *J. Geophys. Res.*, *99*, 3699–3705, 1994.

Volz-Thomas, A., A. Lerner, H.-W. Pätz, M. Schultz, D. S. McKenna, R. Schmitt, S. Madronich, and E. P. Röth, Airborne measurements of the photolysis frequency of NO_2, *J. Geophys. Res.*, *101*, 18,613–18,627, 1996.

Waliser, D. E., N. E. Graham, and C. Gautier, Comparison of the highly reflective cloud and outgoing longwave radiation data set for use in estimating tropical deep convection, *J. Clim.*, *6*, 331–335, 1993.

Wang, C., and P. Crutzen, Impact of a simulated severe local storm on the redistribution of sulfur dioxide, *J. Geophys. Res.*, *100*, 11,357–11,367, 1995.

Wang, C., and R. G. Prinn, On the roles of deep convective clouds in tropospheric chemistry, *J. Geophys. Res.*, *105*, 22,269–22,297, 2000.

Wang, Y., A. W. DeSilva, and G. C. Goldenbaum, Nitric oxide production by simulated lightning: Dependence on current, energy, and pressure, *J. Geophys. Res.*, *103*, 19,149–19,159, 1998a.

Wang, Y., D. J. Jacob, and J. A. Logan, Global simulation of tropospheric O_3-NO_x-hydrocarbon chemistry, 1, Model formulation, *J. Geophys. Res.*, *103*, 10,713–10,725, 1998b.

Winterrath, T., T. P. Kurosu, A. Richter, and J. P. Burrows, Enhanced O_3 and NO_2 in thunderstorm clouds: Convection or production?, *Geophys. Res. Lett.*, *26*, 1291–1294, 1999.

World Meteorological Organization (WMO), Scientific assessment of ozone depletion: 1994, *Rep. 37,* Global Ozone Res. and Monit. Proj., Geneva, 1995.

Yu, F., and R. P. Turco, Ultrafine aerosol formation via ion-mediated nucleation, *Geophys. Res. Lett.*, *27*, 883–886, 2000.

Zhang, R., N. T. Sanger, R. E. Orville, X. Tie, W. Randel, and E. R. Williams, Enhanced NO_x by lightning in the upper troposphere and lower stratosphere inferred from the UARS global NO_2 measurements, *Geophys. Res. Lett.*, *27*, 685–688, 2000.

Zhang, Y., S. Kreidenweis, and G. R. Taylor, The effect of clouds on aerosol and chemical species production and distribution, part III, Aerosol model description and sensitivity analysis, *J. Atmos. Sci.*, *55*, 921–939, 1998.

Ziereis, H., H. Schlager, P. Schulte, I. Köhler, R. Marquardt, and C. Feigl, In situ measurements of the NO_x distribution and variability over the eastern North Atlantic, *J. Geophys. Res.*, *104*, 16,021–16,032, 1999.

Ziereis, H., H. Schlager, P. Schulte, P. F. J. van Velthoven, and F. Slemr, Distributions of NO, NO_x, and NO_y in the upper troposphere and lower stratosphere between 28° and 61°N during POLINAT 2, *J. Geophys. Res.*, *105*, 3653–3664, 2000.

————————

C. Feigl, H. Höller, H. Huntrieser, A. Petzold, H. Schlager, F. Schröder, and U. Schumann, Institut für Physik der Atmosphäre, Deutsches Zentrum für Luft- und Raumfahrt, Oberpfaffenhofen, D-82230 Wessling, Germany. (heidi.huntrieser@dlr.de)

F. Flatøy, Norwegian Institute for Air Research (NILU), P.O. Box 100, N-2007 Kjeller, Norway. (frode.flatoy@gfi.uib.no)

C. Gerbig, Department of Earth and Planetary Science, Harvard University, Cambridge, MA 02138, USA.

C. Théry, Atmospheric Environment Research Section, DMPH/EAG, ONERA, BP 72-29, avenue de la Division Leclerc, 92322 Chatillon, France. (thery@onera.fr)

P. van Velthoven, Section of Atmospheric Composition, Royal Netherlands Meteorological Institute (KNMI), P.O. Box 201, 3730 AEDe Bilt, Netherlands. (velthove@knmi.nl)
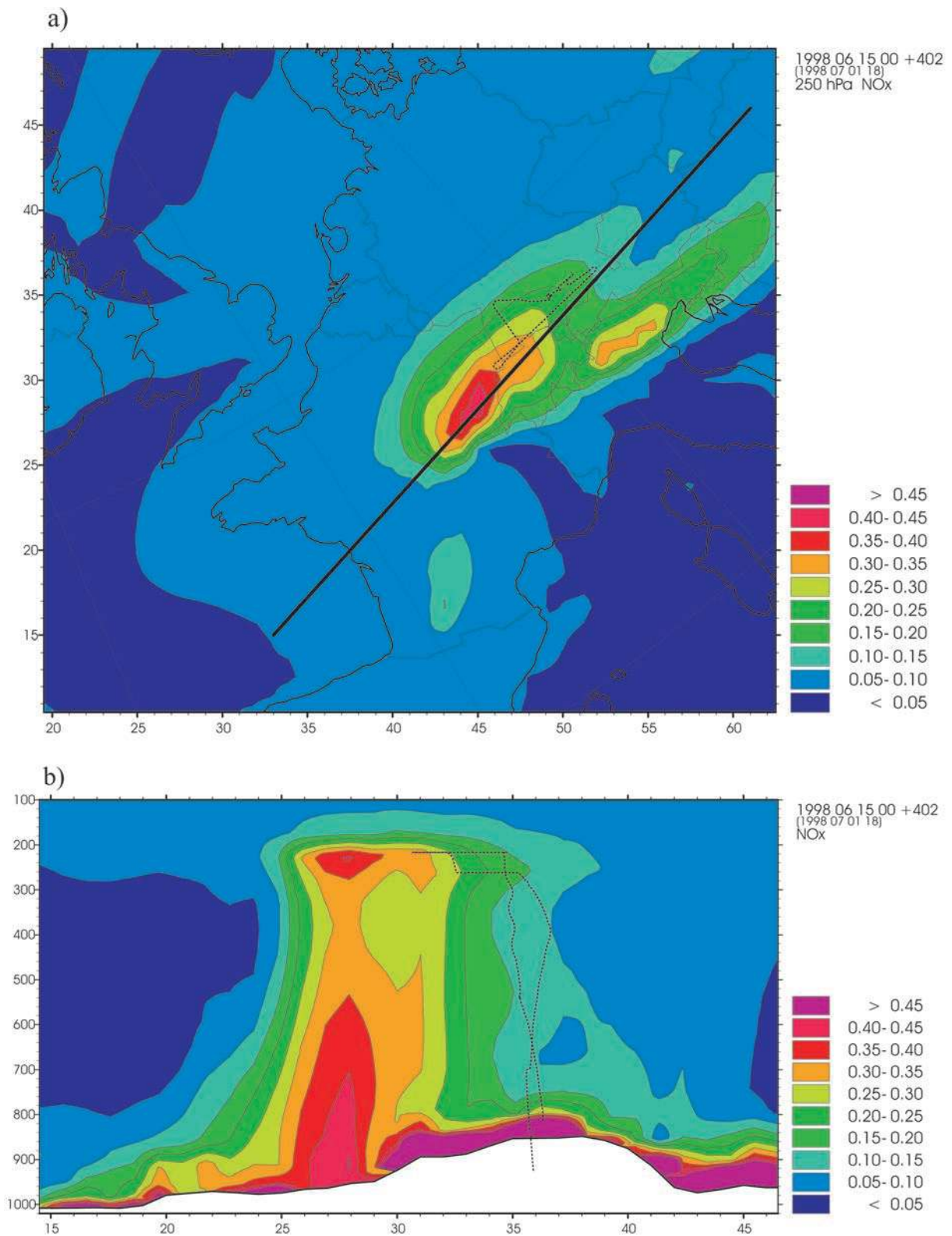
a)

1998 06 15 00 +402
(1998 07 01 18)
250 hPa NOx

![magenta]	> 0.45
![pink]	0.40- 0.45
![red]	0.35- 0.40
![orange]	0.30- 0.35
![yellow-green]	0.25- 0.30
![green]	0.20- 0.25
![green2]	0.15- 0.20
![teal]	0.10- 0.15
![cyan]	0.05- 0.10
![blue]	< 0.05

b)

1998 06 15 00 +402
(1998 07 01 18)
NOx

![magenta]	> 0.45
![pink]	0.40- 0.45
![red]	0.35- 0.40
![orange]	0.30- 0.35
![yellow-green]	0.25- 0.30
![green]	0.20- 0.25
![green2]	0.15- 0.20
![teal]	0.10- 0.15
![cyan]	0.05- 0.10
![blue]	< 0.05

Figure 4. CTM calculation from NILU for 1800 UTC 1 July. (a) Total horizontal NO$_x$ distribution (ppbv) at 250 hPa over western Europe (including lightning-produced NO$_x$). (b) Total NO$_x$ distribution in a cross section along the line indicated in Figure 4a. The dotted lines in all figures indicate the flight track.
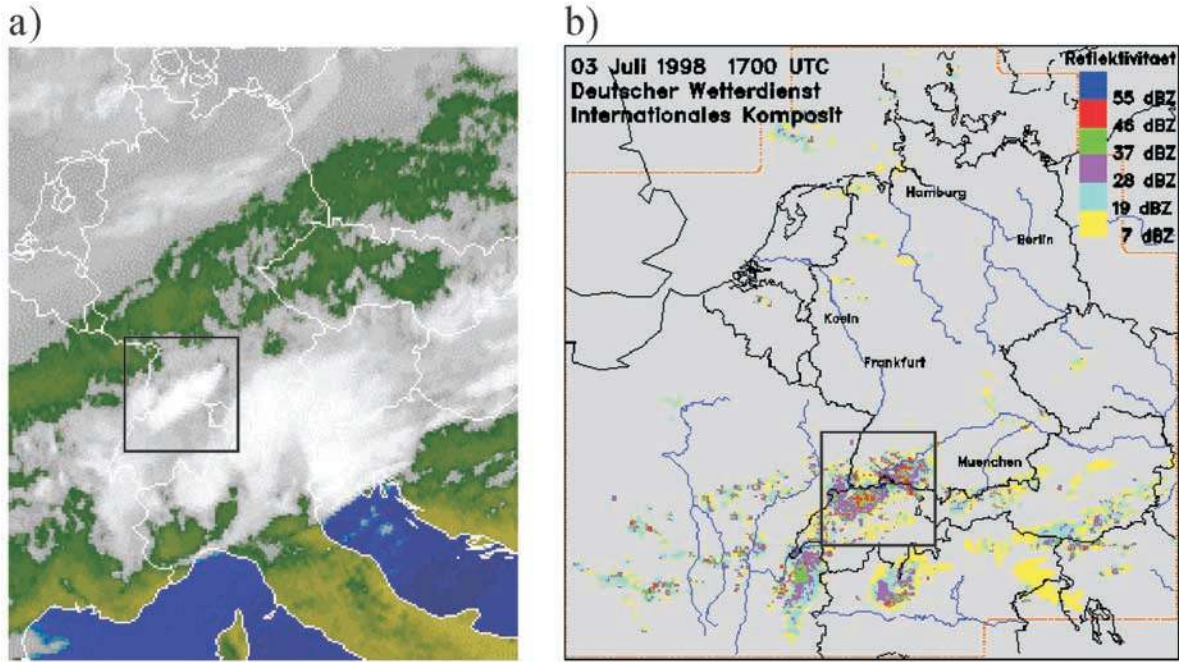
Figure 9. (a) METEOSAT-IR image for 1700 UTC 3 July. The black box indicates the investigated thunderstorms. (b) Radar image for 1700 UTC 3 July from the German Weather Service (DWD). Colors indicate different radar reflectivities (see legend).
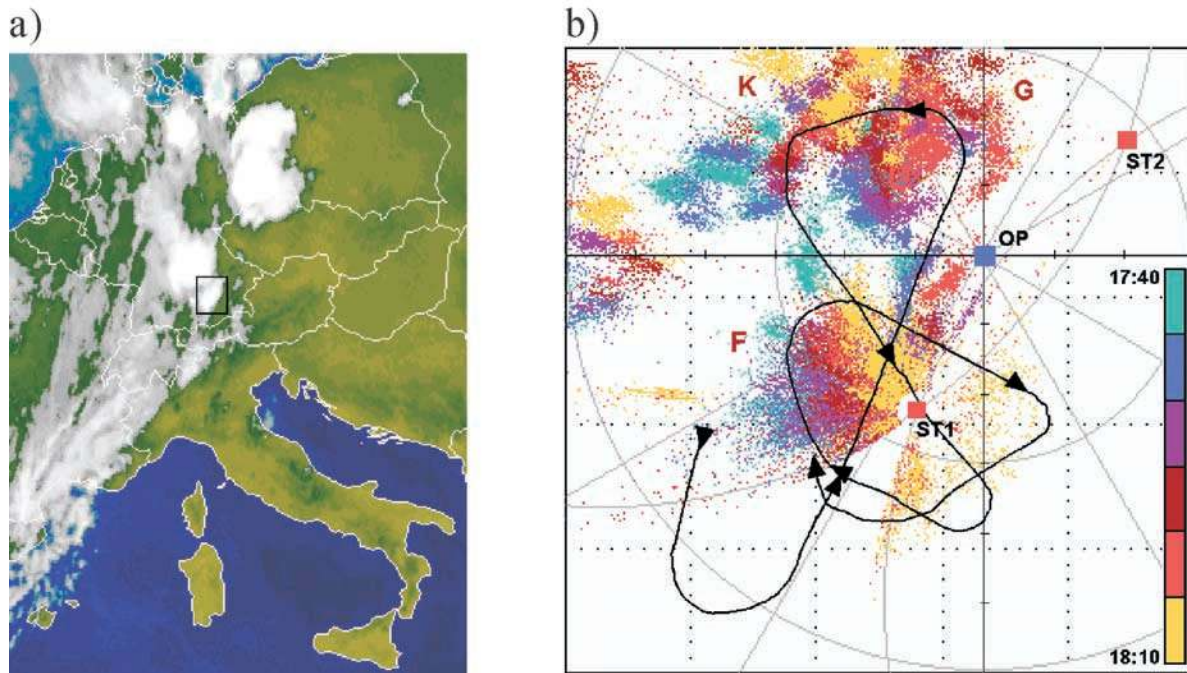

Figure 15. (a) METEOSAT-IR image of central Europe for 1800 UTC, 21 July. The thunderstorm investigated by the in situ measurements is marked by the black box. (b) Ground projection (90 × 90 km) of VHF sources detected by the ONERA system between 1740 and 1810 UTC, 21 July. Each color corresponds to a 5-min period. Red letters, labels of electrical cells; black line, Falcon trajectory during this time (1740–1810 UTC) with an arrow every 5 min; red squares, interferometric stations; blue square, operational center at Oberpfaffenhofen (48°N, 11°E).